

CRITICAL REVIEW

[View Article Online](#)  
[View Journal](#) | [View Issue](#)



Cite this: *RSC Sustainability*, 2025, **3**, 37

## Biodegradable biopolymers for electrochemical energy storage devices in a circular economy

Mustehsan Beg,\* Jeeva Saju, Keith M. Alcock, Achu Titus Mavelil, Prasutha Rani Markapudi, Hongnian Yu and Libu Manjakkal \*

The rising trend of green energy has made it necessary to utilise efficient green materials in electrochemical energy storage devices (EESDs) under a green economy. The need for sustainable energy storage technologies due to the rising demand for energy, improved technology, and the huge challenge of E-waste requires the development of eco-friendly advanced materials and recycling processes in electrochemical energy storage within a circular economy framework. This paper focuses on cellulose, shellac, polylactic acid (PLA), chitin, and chitosan due to their exceptional sustainability, biodegradability, and functional properties and explore how these polymers can improve the circular economy for batteries and supercapacitors by following the aspects of their background, processing and preparation methods, properties, chemical structures, applications, and recent development. As such, this review promotes the increased utilisation of biodegradable biopolymers within the circular economy of EESDs, particularly for future technologies such as flexible, wearable, stretchable, and transparent devices. This review raises awareness of these materials' capability to improve sustainability and recyclability, thus promoting increased use and integration of these materials into EESDs leading to green technologies and low environmental impact.

Received 13th August 2024  
Accepted 6th December 2024

DOI: 10.1039/d4su00468j  
[rsc.li/rscsus](http://rsc.li/rscsus)

### Sustainability spotlight

The recycling of electronic waste (E-waste) is increasingly recognised as a global issue due to its large volume, hazardous nature, and the risk of losing valuable metals. The recycling process involves various physicochemical reactions, and a better understanding of these reactions can improve recycling efficiency. The circular economy provides a solution to the E-waste challenge by emphasising the principles of reducing, reusing, and recycling. In electronics, biopolymers have been used to create eco-friendly components that address the growing issue of E-waste. This paper examines the use of biopolymers in electrochemical energy storage devices.

## 1. Introduction

To achieve economic growth, governments and nations continually expand their industrial activities. This expansion includes increasing manufacturing output, investing in infrastructure development, and improving technological advancements. These industrial activities are essential for boosting productivity, creating jobs, and fostering innovation, all of which contribute to the overall economic prosperity of nations. However, this growth often comes with environmental challenges that must be addressed through sustainable practices and embracing green energy solutions. Adopting renewable green materials reduces the carbon footprint (CF) of production processes, supports local economies, and promotes biodiversity, ultimately contributing to a more sustainable and environmentally friendly future.<sup>1</sup> The ubiquity of electrochemical

energy storage devices (EESDs), such as batteries and supercapacitors (SC), in everyday life underlines their crucial role in a sustainable and environmentally friendly future. These devices enable efficient storage and utilisation of renewable energy while reducing reliance on fossil fuels.<sup>2</sup> Hence, economic growth and environmental well-being is an economic model which reduces the impact of production and consumption on the environment. It also creates a positive relationship between economic development and ecological balance, exemplifying the principles of a green economy.<sup>3</sup>

The recycling of electronic waste (E-waste) is increasingly recognised as a global issue due to its large volume, hazardous nature, and the risk of losing valuable metals.<sup>4</sup> The recycling process involves various physicochemical reactions, and a better understanding of these reactions can improve recycling efficiency.<sup>5</sup> The circular economy provides a solution to the E-waste challenge by emphasising the principles of reducing, reusing, and recycling. This approach focuses on extending product lifecycles through repair, refurbishment, and recycling, thereby minimising waste and recovering valuable materials.<sup>6,7</sup>

School of Computing and Engineering, The Built Environment Edinburgh Napier University, Merchiston Campus, Edinburgh, EH10 5DT, UK. E-mail: [mustehsan\\_beg@napier.ac.uk](mailto:mustehsan_beg@napier.ac.uk); [L.Manjakkal@napier.ac.uk](mailto:L.Manjakkal@napier.ac.uk)



The textile-based electronic devices including sensors and energy storage are also found significant interest in the development of sustainable devices.<sup>8–17</sup> Another approach to reducing E-waste is the development of electronic devices using bio-compatible polymers.<sup>18–21</sup>

Recently, there has been great interest in biopolymer materials for packaging,<sup>22–34</sup> agriculture,<sup>35–42</sup> medical,<sup>43–50</sup> and textile<sup>51–58</sup> due to their potential to reduce environmental pollution, improve sustainability, and offer biodegradable alternatives to conventional plastics. Advances in biopolymer technology have enabled the development of materials with enhanced properties, such as biodegradability,<sup>59,60</sup> increased strength,<sup>61,62</sup> flexibility,<sup>63–65</sup> and thermal stability.<sup>66–68</sup> In electronics, biopolymers have been used to create eco-friendly components that address the growing issue of E-waste. Biodegradable casings for electronic devices,<sup>69–71</sup> such as smartphones and laptops, help reduce the accumulation of non-degradable waste in landfills. Additionally, biodegradable

circuit boards,<sup>72–77</sup> and insulating materials<sup>78–80</sup> are being developed to replace traditional petroleum-based plastics, contributing to a more sustainable electronics industry. EESDs are not far behind with increased use of biopolymers, especially in batteries and SCs.<sup>63,81–87</sup> These biopolymer-based components offer enhanced sustainability and potentially improved performance, supporting the transition to more environmentally friendly energy storage solutions. As research progresses, biopolymers are expected to play a significant role in the development of next-generation energy storage technologies, contributing to reduced environmental impact and enhanced performance.

Not all biopolymers are biodegradable; this paper examines the circular economy of EESDs with a focus on E-waste and recycling processes. Compared to previous reviews on textile-based EESD,<sup>13,88</sup> natural fibres and natural derived polymers based energy storages,<sup>89,90</sup> cellulose-based energy systems,<sup>91,92</sup> this review specifically explores biodegradable biopolymers,



Mustehsan Beg

engineer, and modelling and simulating battery packs for hydrogen fuel cell vehicles for HVS systems.

*Mustehsan Beg, recently completed his PhD thesis at Edinburgh Napier University on flexible energy storage devices, with most of his work focused on the processing of water hyacinth cellulose nanofibers and the synthesis of functional materials such as cellulose-based separators, hydrogels for flexible and wearable energy harvesting and electrochemical energy storage devices. Previous work experience includes being a simulation*



Jeeva Saju

*Jeeva Saju holds dual master's degrees in Advanced Materials Engineering from Edinburgh Napier University, UK, and Analytical Chemistry from Mahatma Gandhi University, India, along with a bachelor's in Chemistry. She has gained valuable experience as a research assistant at Edinburgh Napier University, focusing on energy storage technologies and sensor development.*



Keith M. Alcock

*Dr Alcock holds positions as a researcher at the University of East Anglia and an associate staff member at Edinburgh Napier University. His research interests span battery thermal management systems, fiber optic sensors, and sustainable energy materials, contributing to advancements in energy storage technologies.*

*Dr Keith M. Alcock currently specialises in Lossy Mode Resonance (LMR) optical fiber sensors for energy storage applications. He completed his academic journey at Edinburgh Napier University, earning a PhD in engineering (2023) focused on lithium-ion battery thermal monitoring and management, a Master's in Renewable Energy (2016), and a Bachelor's in Energy & Environmental Engineering (2015).*



Achu Titus Mavelil

*Achu Mavelil Titus, a PhD researcher at Dublin City University, specializes in Multi-material Printing Technology. She holds a bachelor's degree in electrical and Electronics Engineering from APJ Abdul Kalam Technological University and a master in Renewable Energy from Edinburgh Napier University. Her research focuses on energy storage devices and sensors.*

such as cellulose, shellac, polylactic acid (PLA), chitin, and chitosan. It covers their background, processing and preparation methods, properties, chemical structures, applications, and recent advancements in the field. By providing a comprehensive overview of these biopolymers, the paper aims to highlight their potential in enhancing the sustainability and recyclability of EESDs. It explores applications such as separators, electrode materials, electrolytes, and binders for integrating these materials into EESDs, thereby advancing the development of green technologies with a lower environmental impact. This approach supports the broader adoption of biodegradable biopolymers, advancing innovation in sustainable design and promoting a circular economy that minimises waste and optimises material utilisation as represented in Fig. 1.

## 2. Circular economy for EESDs

With the rapidly changing climate, dwindling fossil fuel resources, and a projected global population of 9.19 billion by 2040,<sup>93</sup> combined with increasing technological advancements



Prasutha Rani Markapudi

*Prasutha Markapudi, a PhD student at Edinburgh Napier University; her research focuses on electrochemical sensors with a special focus on the development and optimization of high-sensitivity, low-cost sensing systems with improved efficiency and environmental impact particularly in the real-time water quality monitoring field.*



Hongnian Yu

*Dr Hongnian Yu, Professor at Edinburgh Napier University's School of Computing, Engineering, and the Built Environment, focuses on robotics for rescue, recovery, and healthcare, and ICT-enabled healthcare, including assistive technologies for the elderly and people with dementia. He has authored over 200 research papers and secured £10m in grants from EPSRC, the Royal Society, EU, and industry. A Fellow of IET and RSA, and a member of the EPSRC Peer Review College, he has received the F. C. William Premium and gold medals at INNOVA 2009 and the Geneva International Exhibition for his robotic innovations.*

Open Access Article. Published on 10 December 2024. Downloaded on 2/22/2026 7:33:17 AM.  
This article is licensed under a Creative Commons Attribution 3.0 Unported Licence.  
(CC) BY

in areas like the Internet of Things (IoT), artificial intelligence (AI), quantum computing, robotics, neurotechnology, and green transportation, are all driving the need for innovative materials. These include metamaterials, superconductors, smart materials, and advanced polymers that can meet rising energy demands in electronics and other applications while maintaining efficiency, sustainability, and environmentally friendly products for the growing global population to consume.

E-waste refers to equipment that operates using electromagnetic fields and electrical currents, which is no longer wanted, non-functional, or has reached the end of its life.<sup>94</sup> It covers a driver's array of electronic devices, from large industrial equipment to millimetre-sized printed circuit boards (PCBs), and it is the fastest-growing class of waste worldwide.<sup>94</sup> E-waste has a wide range covering over 100 elements from the periodic table, including polymers, ceramics, precious metals (gold, silver, platinum, iridium, ruthenium, rhodium, copper, and osmium), critical raw materials (indium, bismuth, palladium, cobalt, and germanium) and noncritical metals (e.g., iron and aluminium).<sup>95,96</sup> Improper disposal of these toxic elements can result in them seeping into the soil, surfaces, and groundwater, or being released into the air. This can harm public health and the environment.<sup>96</sup> Also, E-waste applications encompass various parts of electronic equipment, such as energy storage devices, electric wires, PCBs, and polymer packages.<sup>95</sup>

To alleviate pressure on the energy storage raw materials supply chain and minimise the environmental footprint, urgent



Libu Manjakkal

*Dr Libu Manjakkal (PhD, MRSC): Libu Manjakkal received BSc (2006), MSc (2008) degrees in physics from Calicut University and Mahatma Gandhi University, India. From 2009 to 2012, he was with CMET, Thrissur, India and in 2012 he worked at NOVA School of Science and Technology in Lisbon, Portugal. He completed a PhD in electronic engineering from the Institute of Electron Technology, Poland (2012–2015) (Marie Curie ITN*

*Program). Between 2016 and 2022, he was a post-doctoral fellow at the University of Glasgow in various roles. Currently, he is a lecturer at Edinburgh Napier University with a research focus on material synthesis, wearable energy storage, electrochemical sensors, supercapacitors, electrochromic energy storage and energy-autonomous sensing systems. He has authored/co-authored more than 75 peer-review papers (55+ journals). He was shortlisted for important awards such as the European Commission for Marie Curie Awards in the "Promising Research Talent" category, the "Outstanding Young Scientists Scholarship Award" from the Polish Ministry of Higher Education and the RIENG 2024 Young Investigator Award. He is currently the editor of Chemical Engineering Journal and Results in Engineering Journal, Elsevier.*

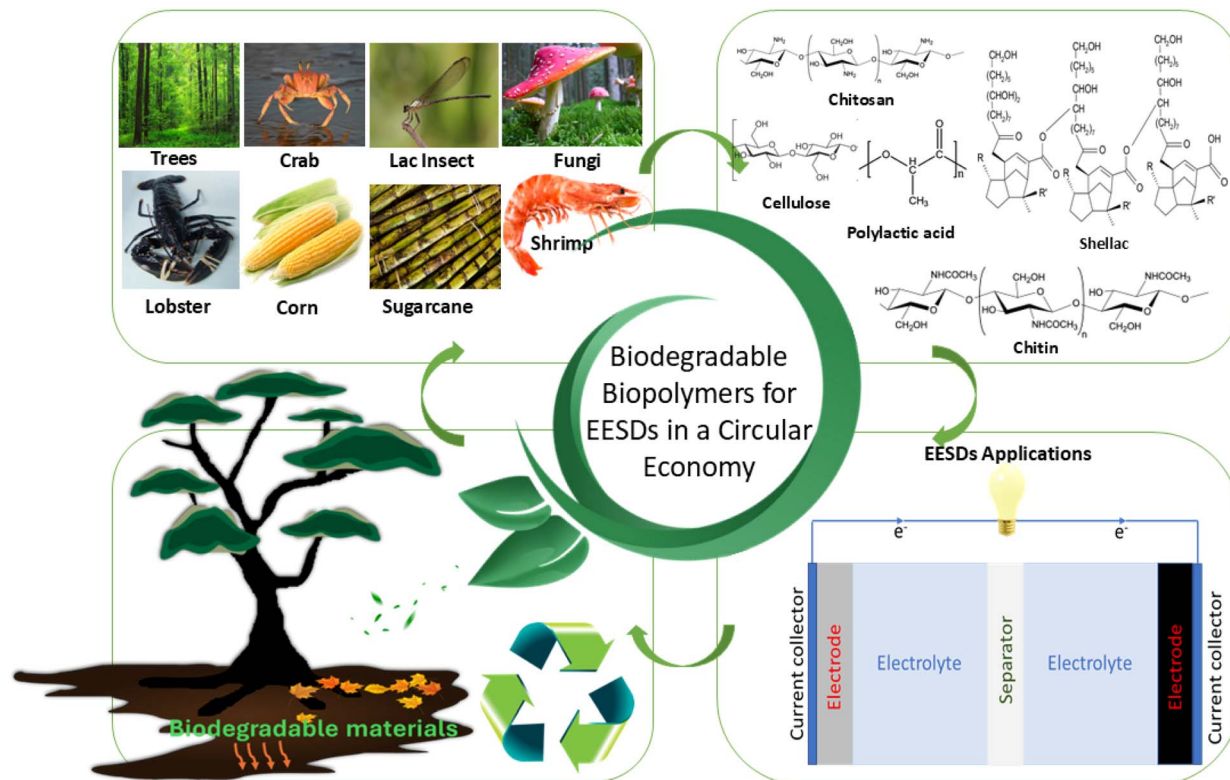


Fig. 1 Biodegradable biopolymers for sustainable design of energy storage.

steps have been implemented across society. Transitioning to a closed-loop model for manufacturing EESDs, such as batteries and SCs, emerges as the ultimate solution for recycling EESDs.<sup>97</sup> Recently, there has been a significant push toward recycling EESDs, such as tantalum capacitors,<sup>98,99</sup> batteries,<sup>97,100–102</sup> and SC<sup>103–105</sup> due to their use of toxic materials. As a result of this, many new companies and start-ups recycling EESDs have opened in the last 15 years, and some of them are listed in Table 1.

There are three main processes used to recycle EESDs, especially Li-ion batteries (LIBs), namely direct, pyrometallurgical, and hydrometallurgy recycling processes. Initially, the LIBs must be classified and pre-treated through discharging,

disassembled, and separated before proceeding to the recycling/reuse processes.<sup>106</sup>

(a) Direct methods involve the disassembly of LIBs and removing of the battery's cathode material, primary consisting of lithium cobalt (LCO) and lithium iron phosphate (LFP) materials for reuse or reconditioning. Meanwhile, work on automating and widening the scope of disassembly is still limited.

(b) Pyrometallurgy involves the shredding or crushing of EESDs and using smelting under a vacuum or inert atmosphere to make a metal alloy consisting of materials used in the EESDs. However, this method is most efficient when applied to valuable metals like cobalt.

Table 1 Some of the recently started companies and start-ups for recycling EESDs

Company name	Headquarters	Established
Li-cycle Corporation	Toronto, Canada	2016
American Battery Technology Company	Nevada, USA	2011
Lithion Recycling Inc.	Montreal, Canada	2018
Redwood Materials, Inc.	Nevada, USA	2017
The Battery Recycling Company	UK	2022
Technology Material	UK	2020
Green Li-ion Pte Ltd	Singapore	2020
Battery Pollution Circunomics	Australia	2022
Botree Cycle	Germany	2019
	China	2019



(c) Hydrometallurgical pre-treatment involves removing the materials from the current collectors and using an aqueous-based solution such as HCl, H<sub>2</sub>SO<sub>4</sub> or organic acids like citric acid to extract and separate. Once metals are extracted in solution, they can be separated by either causing them to precipitate as salts or extracting them using organic solvents.

Globally, in 2019 only 17.4% of E-waste was collected and recycled, while the other 82.6% discarded in an environmentally harmful way such as incineration and landfills.<sup>107</sup> This emphasises the pressing necessity to prioritise the adoption of environmentally friendly and biodegradable biopolymers whenever feasible. Efforts in this direction can contribute significantly to mitigating the adverse environmental impacts associated with improper E-waste disposal.

Currently, most electrochemical cells are manufactured in the continent of Asia.<sup>107</sup> To strengthen Europe's competitiveness in this field, the European Commission has launched an international strategy known as the European Battery Alliance (EBA) and Strategic Energy Technology Plan (SET-Plan). The main aim of EBA is to make Europe self-sufficient in manufacturing and recycling electrochemical cells and the key action of (SET-Plan) is to promote research and development activities for electrochemical cells. Additionally, within a new European regulatory framework, there is a mandatory requirement for the minimum content of certain materials (such as lithium, and cobalt) inside a cell to ensure environmental sustainability.<sup>108</sup> Also, to help consumers make informed decisions about battery purchases, key data will be provided on a label *via* a QR code. This QR code will grant access to a digital passport containing detailed information about each battery, aiding consumers and professionals along the value chain in their efforts to realise the circular economy for EESDs.<sup>109</sup>

The increased use of polymers in EESDs and other products has quadrupled plastic production, leading to a significant rise in greenhouse gas emissions, expressed as carbon dioxide equivalents (CO<sub>2</sub>e), generated throughout its lifecycle, and is projected to account for 15% of the global carbon budget by 2050.<sup>110</sup> The CF of cellulose varies depending on its source, such as wood or agricultural waste, and its processing methods. Natural cellulose polymers generally have a much lower footprint compared to synthetic polymers. However, mechanical, and chemical pulping methods are energy-intensive, and advanced processes for nanocellulose, further increase energy consumption. Nanocellulose typically has a global warming potential (GWP) ranging from 18.6 to 1160 kg CO<sub>2</sub>e per kg at the laboratory scale and 5.6 to 16.8 kg CO<sub>2</sub>e per kg at the industrial scale. These values reflect the significant differences in energy consumption and efficiency between experimental setups and large-scale production processes.<sup>111</sup> Another study showed the CF of manufacturing of chitosan-CNF composite films is approximately 3.91 kg CO<sub>2</sub>e per kg of the film, which is slightly lower than that of fossil-based low-density polyethylene (LDPE) and bio-based poly(lactic acid) (PLA) films.<sup>112</sup>

Chitin and chitosan, which are derived from crustacean shell waste, are low-emission materials. However, the chemical treatments involved in their extraction, such as alkaline or acidic processes, contribute to their CF. Harvesting crustacean

shells from seafood processing incurs negligible additional carbon costs, but the demineralisation and deproteinisation processes require energy and chemicals. A study showed two scenarios for chitosan production: in scenario (1), the supply chain involves processing snow crab in Canada, shipping dry shells to China for chitin production, and sending the chitin to the Netherlands for chitosan processing, resulting in a greenhouse gas (GHG) footprint of 134.9 kg CO<sub>2</sub>e per kg. In scenario (2), shrimp caught in the Arabian Sea and processed nearby has a much lower footprint of 20.6 kg CO<sub>2</sub>e per kg. The sensitivity analysis revealed that chitosan yield significantly impacts GHG emissions, with a 15% yield in Norway (using Norway electricity production patterns) leading to 72.5 kg CO<sub>2</sub>e per kg, while a 5% yield increases the footprint to 217.6 kg CO<sub>2</sub>e per kg. In contrast, the Portugal alternative (using Portugal electricity production patterns), with a 15% yield, has a GHG footprint of 207.8 kg CO<sub>2</sub>e per kg, which rises to 623.3 kg CO<sub>2</sub>e per kg with a 5% yield. These results highlight that lower chitosan yields require more resources, thus increasing GHG emissions. The best alternative, using conventional eco-solvents with 40 wt% NaOH, considering the electricity source and chitosan yield, was found to have the lowest GHG footprint among the alternatives, emphasising the importance of production processes in reducing environmental impacts.<sup>113</sup> Another study on the cradle-to-gate impacts of chitin nanofibril extraction from fungi compared its environmental effects to conventional chitin nanocrystal hydrolytic isolation processes from shrimp shells, chitin powder, crab shells, and the sulfuric acid-induced hydrolysis of microcrystalline cellulose to cellulose nanocrystals. The analysis, which scaled laboratory quantities to processes treating 1 kg of biowaste, revealed that the global GWP of 18.5 kg CO<sub>2</sub>e per kg of chitin nanofibrils was significantly lower than the GWP values of 906.8 kg CO<sub>2</sub>e per kg for chitin nanocrystals from shrimp shells, 105.2 kg CO<sub>2</sub>e per kg for chitin powder, 543.5 kg CO<sub>2</sub>e per kg for crab shells, and 177.9 kg CO<sub>2</sub>e per kg for cellulose nanocrystals.<sup>114</sup>

PLA is considered a sustainable alternative to petroleum-based plastics; however, its production comes with moderate CF due to the energy-intensive processes of fermentation and polymerisation. Additional emissions result from the cultivation of feedstocks like corn or sugarcane, which require fertilisers, and irrigation, and may lead to land-use changes, further contributing to its environmental impact. The CF and 100 years Global Warming Potential (GWP100) associated with the life cycle of polylactic acid (PLA) trays for fresh food packaging were assessed, with a comparison to polystyrene (PS)-based trays. Two transportation scenarios were considered for the supply of PLA granules to the tray production facility: a transoceanic freight vessel and an intercontinental freight aircraft. The study revealed that the GWP100 is mainly driven by the production of PLA granulate and its transportation to the manufacturing site. Depending on the transportation method, the CF associated with the PLA trays can increase to the point where they are no longer more GHG emission efficient compared to PS trays. The GWP100 for the system analysed was 4.826 kg CO<sub>2</sub>e per kg of packed trays, with the production of PLA granulate accounting for 61.26% of the impact. The study showed that the GWP100 of



EPLA trays (4.826 kg CO<sub>2</sub>e) is only slightly lower than that of EPS trays (5.11 kg CO<sub>2</sub>e), indicating a small difference of 5.5% between the two types of trays.<sup>115</sup> Shellac, on the other hand, has a relatively low CF compared to synthetic resins because it is a natural product derived from the secretion of lac insects. The primary emissions associated with shellac result from harvesting and processing lac, which often involve manual and low-energy methods commonly used in countries like India and Thailand. Transportation of raw lac and processed shellac also contributes to emissions. There is limited information available on the GWP of shellac, which could make it an interesting area for future research.

### 3. Biodegradable EESDs biopolymers

Materials play a crucial role in the circular economy of EESDs. The use of biodegradable materials can help maintain cell durability, preventing misuse and ensuring sustainability within the circular economy framework. By incorporating biodegradable materials, energy storage devices can be designed to minimise environmental impact, facilitate easier recycling, and reduce the reliance on non-renewable resources. This approach not only supports the responsible management of end-of-life devices but also promotes the development of more sustainable and eco-friendly energy storage solutions. While biodegradable metals are a topic of research primarily in medical applications (e.g., magnesium-based alloys for biodegradable implants),<sup>116</sup> they are not yet viable for use in EESDs.

Recent research has increasingly focused on materials such as biodegradable biopolymers in EESDs (batteries and SC). While there are various biodegradable biopolymers used in EESDs, this paper will focus on cellulose, shellac, PLA, chitin, and chitosan due to their exceptional sustainability, biodegradability, and functional properties. Fig. 2(a) and (b) display the results from Google Scholar and ScienceDirect between 2020 and 2024, showing the total number of search results in their databases related to specific input keywords (e.g., in Google Scholar, the input keywords “cellulose” AND “battery” were used to determine the number of results for cellulose in Fig. 2(a) and so on). The data clearly indicate that cellulose and chitosan are the most widely used biodegradable biopolymers, while shellac is underused for both battery and SC. Fig. 2(c) and (d) demonstrate the increased use of these biodegradable biopolymers in both batteries and SC between 2019 and 2023.

#### 3.1. Cellulose

Cellulose is the most abundant organic compound on earth, boasting a global production of approximately 1.5 (ref. 12) tonnes, and it has been in use for over 150 years.<sup>117</sup> Apart from its enduring scientific appeal, the utilisation of cellulose as a renewable, biodegradable biopolymer raw material across various applications emerges as a proposed solution to address industrial challenges associated with environmental concerns and recycling issues.<sup>118</sup> The versatile structure of cellulose by modification, including chemical, physical and hybrid

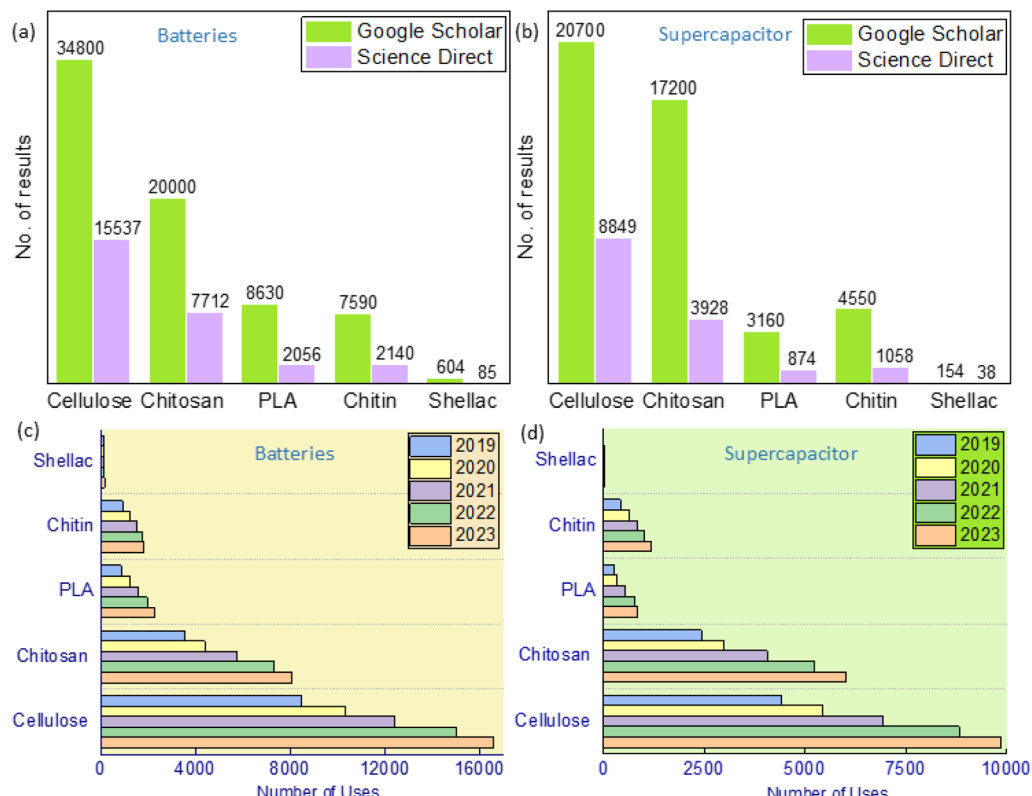


Fig. 2 Databases related to published work of biopolymers based (a) batteries (b) SC and its number of uses materials between 2019 and 2023 in (c) batteries and (d) SC.

methods, has enabled its use in wide variety of applications, such as biodegradable plastics, fillers, binders, coating, paper, textile, food industry, medical applications, cosmetics, building materials, optical films, and even in advanced functional materials.<sup>119</sup> There are various processes used to extract cellulose, including alkaline, bisulphite, sodium hypochlorite, and sulphite, in combination with thermal and mechanical treatments, which produces various fibre strengths from the cellulose pulp.<sup>120</sup> Furthermore, advanced micro and nano structure of cellulose can be achieved through physical and hydrolytic treatments. Cellulose's versatility and abundance makes it a highly desirable and sustainable material, contributing significantly to the fields of biomaterials, biochemistry, and green chemistry.

Cellulose is present in various sources, including plants, animals, algae, fungi, and minerals.<sup>121–125</sup> However, plant fibre remains the primary source of cellulose. It serves as a strengthening element in the cell wall, providing optimal support and strength to plants, comprising of around 40% of the carbon content in plants.<sup>118</sup> While cellulose can exist in its pure form in plants, it is commonly associated with hemicelluloses, lignin's, and relatively minor quantities of extractives, such as resins, oils, alcohols and fatty acids.<sup>118</sup> The cellulose content in various plant-based feedstocks depends on the specific type and part of the plant, such as stem, straw, seed, or leaves *etc.* For example, the lint of cotton bolls that are used in making cotton cloth, is mostly pure cellulose up to 98%, while cotton linters used in manufacturing paper are the short cellulose fibres (1/8 inch long) left on the cotton seed make up to 77% of cellulose.<sup>122,123</sup> Table 2 shows some plant-based cellulose sources and their cellulose, hemicellulose, and lignin contents.<sup>121–126</sup>

Cellulose is a polysaccharide of  $\beta$ -D-anhydroglucopyranose ( $C_6H_{10}O_5$ ), meaning a carbohydrate (sugar) formed by long chains of repeating units linked together by glycosidic bonds. It is composed of a linear chain containing several hundred to several thousand glucose units linked together by a beta bond between the first and fourth carbon atoms of the glucose molecules. This bond is also known as a  $\beta$  (1 → 4) linked D-glucose units. Fig. 3(a) represents the structure of cellulose chain illustrating the anhydroglucopyranose unit in the chair conformation, including atom numbering, the glycosidic link, and

both the reducing properties and non-reducing ends of cellulose. Cellobiose unit refers to two glucose molecules linked by a  $\beta$  (1 → 4) glycosidic bond.<sup>127</sup> The linear structure of cellulose, reinforced by strong hydrogen bonding between chains, imparts high mechanical strength, while the abundant hydroxyl groups (–OH) on its chains allow for chemical modifications that enhance conductivity through functionalisation with conductive polymers or metal nanoparticles, improve ion transport by interacting with electrolyte ions, and, when processed into a porous form, increase the surface area available for electrochemical reactions, all of which significantly boost its performance in energy storage devices such as SCs and batteries.

Cellulose molecules can have a wide range of chain lengths. The  $n$  in the anhydroglucopyranose unit refers to the degree of polymerisation, it is the number of individual glucose units linked together in a cellulose chain. It is a measure of the polymer chain length and shows how many monomeric units are present in the polymer.<sup>127</sup> Three hydroxyl groups (OH) located at the C2, C3, and C6 positions in equatorial positions in the  $\beta$ -D-anhydroglucopyranose units in cellulose.<sup>131</sup> The hydroxyl groups on the cellulose backbone, acting as reactive sites, feature a primary alcohol at C6, which is less hampered and more reactive compared to the secondary alcohols at C2 and C3. Semicrystalline material such as cellulose is made from series of strong intramolecular hydrogen bonding reactions and intermolecular hydrogen bonding interactions amid the  $\beta$ -D-anhydroglucopyranose units and hydroxyl groups grants cellulose chain with high strength and hydrophilic properties.<sup>132</sup>

The raw material, wood, after the removal of bark, undergoes chipping. Then, the wood chips are screened to achieve uniform sizes, washed, and temporarily stored until they are introduced into the pulping mill.<sup>133</sup> Pulps are fibre-based material from plants dry matter, also known as lignocellulosic biomass, which is mainly composed of cellulose, hemicellulose, and lignin.<sup>134</sup> The amount of non-cellulose components highly depends on the extraction method, these pulping methods includes chemical pulping, semi-chemical pulping, mechanical pulping, and chemi-mechanical pulping.<sup>133</sup> Mechanical pulps retain a substantial percentage (85–95%) of the original wood components in the final product, providing evident economic benefits. However, the process unavoidably inflicts damage to

Table 2 Cellulose, hemicellulose, lignin contents from different sources

Sources	Cellulose (%)	Hemicellulose (%)	Lignin (%)	Ref.
Hemp	76	11	7	121
Cotton linters	77	5	0.7	122
Cotton fibres	98	0.5	0.4	123
Jute	68	15	11	124
Banana fibre	70	20	8	
Wheat straw	43	34	22	125
Soy hulls	56	13	18	
Corn stover	33	21	19	126
Norway spruce (softwood)	49	20	29	
Hemp	63	10	6	



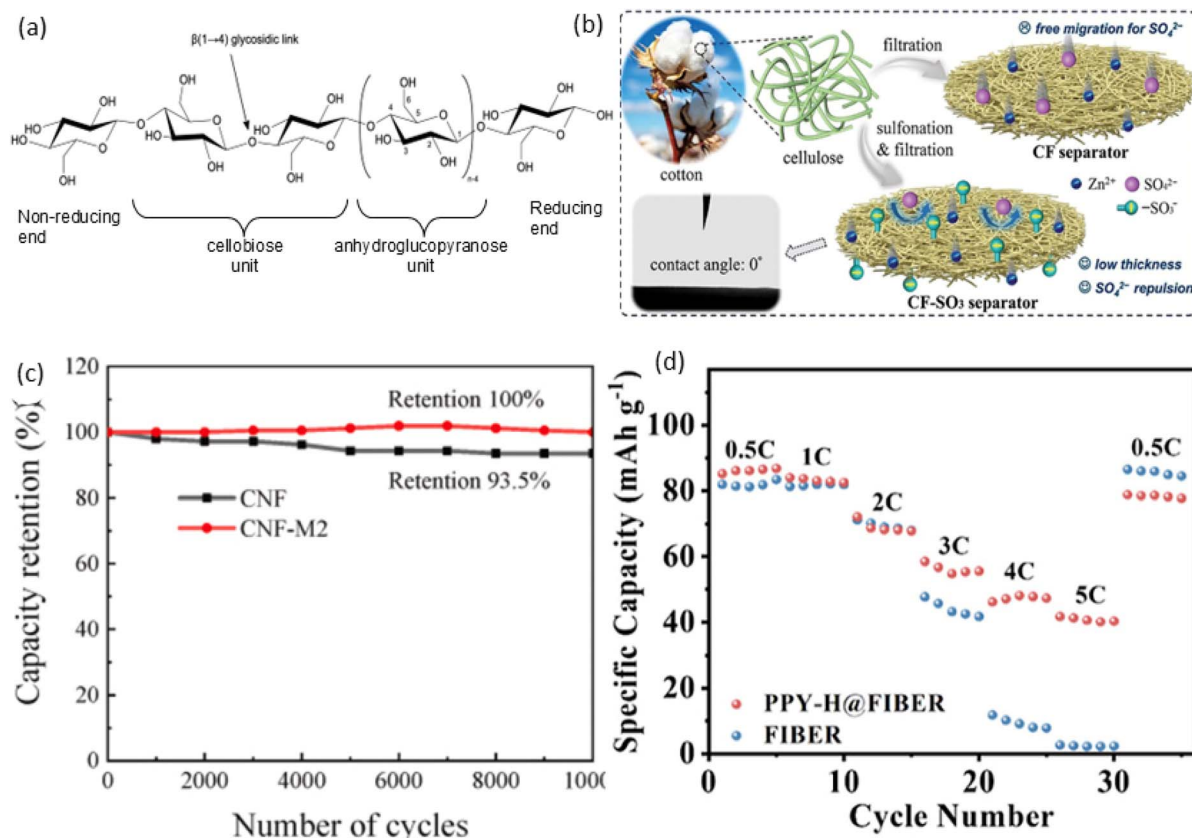


**Fig. 3** (a) Chemical structure of cellulose,<sup>127</sup> (b) sulfonation strategy modification of the cellulose separator, reproduced with permission from John Wiley & Sons, ref. 128, copyright 2024 (c) PDADMAC modified CNF separator maintained 100% capacitance retention over 1000 cycles, reproduced with permission from Elsevier, ref. 129, copyright 2024 and (d) PPY-H@FIBER modification showed specific capacity of  $86.1 \text{ mA h g}^{-1}$  at 0.5C, reprinted with permission from, American Chemical Society, ref. 130 Copyright 2024.

the cellulose fibres, with high lignin content, leading to a lower strength and discolouration over time.<sup>133</sup> Chemical pulping eliminates as much lignin and extractives as possible, preserving high cellulose fibre content as possible. This process typically yields a lower output (40% and 55% of the original wood components), making it more costly compared to mechanical methods.<sup>133,135</sup> In the global pulp production processes for paper 79% is by chemical pulping, 15% are mechanical and semi-chemical pulping and others are remaining 6%. The data indicates that the chemical method holds the major share at 79%.<sup>136</sup> Table 3 compares the two primary pulping processes, namely mechanical and chemical pulping processes.<sup>137</sup>

Nanocellulose is derived from cellulose, within the nanometre scale, specifically with one of its dimensions ranging

3 nm to 100 nm. Cellulose nanofibers (CNF) were initially termed micro-fibrillated cellulose and were first reported in 1983 by Gaulin laboratory homogeniser. Typically, CNF has a diameter between 10 to 40 nm and lengths up to several micrometres, generally extracted from weaker acids like oxalic acid, acetic acid, or low concentrations of sulfuric, nitric, and hydrochloric acids.<sup>138</sup> The degree of polymerisation can be as high as 15 000 depending on the source of cellulose, for example, wood cellulose polymerisation is approximately 10 000, while cotton cellulose has a high degree of polymerisation of 15 000.<sup>138</sup> Cellulose nanocrystals (CNC) have a needle-like structure with a diameter between 3 to 5 nm and length of 100 to 300 nm. They are generally extracted by strong acids such as hydrochloric acid, nitric acid, sulphuric acid, oxalic acid and hydrobromic acid *etc.* at high concentration.<sup>138</sup> The utilisation of strong acids in the CNC extraction process led to the degradation of a significant portion of the amorphous region within the fibre chain resulting in higher crystallinity when compared to CNF.<sup>138</sup> Bacterial cellulose (BC) has an advantage of being free of foreign substances such as lignin and hemicellulose *etc.* The cellulose extracted from bacteria are in the form of ribbon shaped and has a length of <100 nm and width of 2 to 4 nm. The degree of polymerisation is approximately 4000 to 8000 with up to 80% crystallinity.<sup>138</sup> In general, nanocellulose can be

**Table 3** Comparison of pulping processes

	Mechanical pulp	Chemical pulp
Energy consumption	1000 kW per ton of pulp	Self-sufficient
Percentage yield	95%	45%
Fibre length	Short	Long
Paper strength	Low	High
Production cost	Low	High



categorised into two main types: plant and bacterial based, both of which are environmentally friendly and naturally occurring. Over the past decade, numerous research groups worldwide have reported the extraction and utilisation of CNF, CNC, and BC with diverse dimensions and characteristics. The choice of nanocellulose is closely linked to its intended application. The specific type of nanocellulose plays a crucial role in determining its suitable applications. For example, CNF are adept at forming high-quality films, making them suitable as matrices for nanocomposites.<sup>138</sup> On the other hand, cellulose nanocrystals, with their superior crystallinity, find utility as binders in applications like EESDs. Recent advancements have introduced new types of nanocellulose, including cellulose hollow structures derived from cellulose acetate, possess a hollow structure that enhances conductivity in EESDs, hairy cellulose nano crystalloids, and regenerated cellulose.<sup>139–141</sup>

In EESDs, cellulose in the form of carboxymethyl cellulose (CMC) is commonly used as an electrode binder and electrolyte.<sup>142–147</sup> More recently, research has focused on using cellulose nanofibers (CNF) as a main material for separators to replace oil-based polyethylene (PE). In a study on the processing and characterisation of water hyacinth cellulose nanofibers (WHCNF) separators through freeze-thawing, it was shown that a high WHCNF content (95 wt%) enhanced the separator's porosity, electrolyte uptake, and wettability. This makes WHCNF a promising and sustainable option for separator materials.<sup>148</sup> The bilayer separator is produced through a two-step fabrication process that includes freeze-thawing and nonsolvent-induced phase separation. The resulting bilayer separator demonstrates superior properties, with a porosity of 46%, a wettability of 46.5°, and an electrolyte uptake of 194%, outperforming the Celgard 2320 trilayer separator, which has a porosity of 39%, a wettability of 55.58°, and an electrolyte uptake of 110%.<sup>149</sup>

A sulfonation strategy modifies the cellulose separator as shown in Fig. 3(b) (ref. 147) with  $-\text{SO}_3^-$  groups, which inhibit  $\text{SO}_4^{2-}$  migration *via* electrostatic repulsion, increasing the  $\text{Zn}^{2+}$  transference number from 0.44 to 0.60. These groups also facilitate  $\text{Zn}^{2+}$  desolvation and limit planar diffusion at the electrode surface, while the homogeneous nanochannels ensure uniform electric field distribution, promoting dendrite-free Zn deposition and reducing interfacial side reactions. Resulting in a sulfonated cellulose separator with a thin profile of 50  $\mu\text{m}$ , exceptional wet mechanical strength of 18.7 MPa, and high ionic conductivity of 52.1  $\text{mS cm}^{-1}$ . Additionally, the separator effectively promotes dendrite-free Zn deposition and suppresses interfacial side reactions. Consequently, Zn//Zn cells using this separator demonstrate remarkable cycling durability, with extended lifespans of 2500 and 1200 hours at 1 and 4  $\text{mA h cm}^{-2}$ , respectively.<sup>128</sup> A polyacrylonitrile and cellulose composite film is designed using electrospinning, featuring a double-layer fibre configuration, with the outer layer primarily composed of cellulose and the inner layer of polyacrylonitrile. This design enhances the cycling and rate performance of Li-S batteries. The battery's cycle life can be maintained over 200 cycles with a high sulphur loading of 9.1 mg, with the initial area capacity decreasing from 5.67  $\text{mA h cm}^{-2}$  to

4.0  $\text{mA h cm}^{-2}$ .<sup>150</sup> The surface of cellulose nanofibers (CNFs) is modified with a cationic polyelectrolyte, specifically polydiallyldimethylammonium chloride (PDAMAC), to produce a nearly-neutral surface charge CNF membrane derived from rice straw. TEMPO-oxidized CNFs from rice straw were coated with varying amounts of PDADMAC, forming a thin layer on the fibrils. The carboxylate groups from the oxidation created a highly negative zeta potential, which was neutralised by the positively charged PDADMAC, resulting in nearly zero surface charge. PDADMAC also improved porosity, boosting ionic conductivity and electrolyte uptake. The resulting SC, utilising the modified CNF separator, demonstrates an improved specific capacitance of 185.3  $\text{F g}^{-1}$  and a 1.2-fold increase in energy density. Additionally, it maintains 100% capacitance retention over 10 000 cycles as shown in Fig. 3(c).<sup>129</sup> Fabricated a paper separator by simple approach by customising the thickness (approximately 40  $\mu\text{m}$ ), air permeability (0.1–200  $\text{cm}^3 \text{s}^{-1}$ ), and mechanical properties of separators by incorporating up to 50 wt% microfibrillated cellulose (MFC) into paper sheets. MFC enhances the formation of dense networks but exhibits poor dimensional stability and low strength under wet conditions, by crosslinking with 1,2,3,4-butanetetracarboxylic acid increased wet strength by up to 6700%, ensuring dimensional stability. The electrochemical performance, evaluated through impedance spectroscopy and galvanostatic cycling of 7500 cycles, demonstrated comparable results to commercially available glass and polypropylene separators.<sup>151</sup> An *in situ* polymerisation approach was adopted to modify the cellulose separator with polypyrrole using high-temperature-synthesized PPY-H@FIBER and low-temperature-synthesized PPY-L@FIBER samples. PPY-H@FIBER modification enhanced ion conductivity while reducing electron conductivity, improving electrolyte affinity and sodium ion transport. The resulting functional separator exhibits a high sodium ion transfer number (0.62), high ion conductance (2.77  $\text{mS cm}^{-1}$ ), specific capacity of 86.1  $\text{mA h g}^{-1}$  at 0.5C as shown in Fig. 3(d) and uniform sodium ion flux for sodium-based batteries.<sup>130</sup> To ensure uniform Li<sup>+</sup> transport and inhibit lithium dendrite growth, a polydopamine-modified cellulose membrane was developed by oxidative self-polymerising dopamine and bonding it to the surface and interface of the cellulose membrane through hydrogen bonds. The results showed that the membrane exhibited no shrinkage at 160 °C, had a tensile strength of 31.1 MPa, uniform pores with a porosity of 54.95%, homogeneous Li<sup>+</sup> flux, an electrolyte uptake rate of 469.77%, electrolyte retention of 409.04%, a contact angle of 18.35°, ionic conductivity of  $1.54 \times 10^{-3} \text{ S cm}^{-1}$ , and impedance (849  $\Omega$ ). The lithium metal battery utilising the separator demonstrated strong cycling performance, maintaining a high capacity retention rate of 90.48% after 100 cycles.<sup>152</sup>

### 3.2. Shellac

Shellac is a hard, brittle, resinous solid that exhibits no odour when cold but develops a distinct smell when warm.<sup>153</sup> As a natural resin with attractive properties such as amphiphilicity, pH responsiveness, biocompatibility, and biodegradability.<sup>154</sup> It



is secreted by tree insects (*Laccifer Lacca*) especially in Burma, India, Thailand, and southern China and composed of cyclic terpene acids linked by ester bonds and aleuritic acid, providing hydrophilic and hydrophobic segments.<sup>155</sup> Shellac is a refined form of lac resin, derived from insects on trees like palash, ber, kusum, and semialata.<sup>153</sup> Its non-toxic, eco-friendly nature makes it valuable in 3D printing, medical, food industry, pharmaceutical, tissue engineering and the preparation of pH-responsive hydrogel applications.<sup>153</sup> The major components of raw lac are resin, dye, and wax. Its colour spectrum is broad, ranging from pale yellow to deep red.<sup>153</sup> This colour variation is due to several factors, including the type of tree the lac insects feed on, the region where it is harvested, and the method of processing. Lighter shades of shellac wax are often chosen for lighter woods, while darker shades are used to enhance the richness of darker woods or to create an antique appearance. The colour can also be adjusted through various bleaching processes to meet specific requirements for different applications.<sup>153</sup>

Shellac is an amphiphilic biomacromolecule characterised by a distinctive molecular structure composed of aleuritic acid and various cyclic terpene acids (Fig. 4(a)).<sup>153</sup> Depending on the differences between the *R* and *R'* alkyl groups, the cyclic terpene acid moiety in shellac can be aleuritic acid, shellolic acid, jalaric acid, laccolic acid, laccophilic acid, lecophilic acid, lecophilic acid, lecocoliphilic acid, and lecocoliphilic acid.<sup>153</sup>

The aleuritic acid and cyclic terpene acids are linked by ester bonds and act as the hydrophobic and hydrophilic components of the shellac, respectively.<sup>154</sup> The quantity and formation of lactide and ester linkages between aleuritic acid and jalaric acid result in either a high molecular weight fraction, producing a hard resin, or a low molecular weight fraction, producing a soft resin.<sup>159</sup> These acids were extracted using the lac resin by many chemical processes such as oxidation, hydrolysis, and esterification. The geometry of both acids along with their other possible combinations for the formation of diester and trimers. The aleuritic acid has three -OH groups and one -COOH group and jalaric acid has one -COOH, one -CHO and one primary -OH and one secondary -OH groups.<sup>159</sup> Shellac's structure–property relationship in electrochemical energy storage devices is based on its unique molecular structure. Shellac is composed of natural resin with long polymer chains and functional groups, such as hydroxyl and carboxyl groups, that can be chemically modified to enhance its electrochemical properties. These groups provide potential sites for ion transport and interaction with conductive materials. Additionally, shellac's rigidity and film-forming ability contribute to its mechanical stability, making it suitable for use as a binder or coating in electrodes. However, its

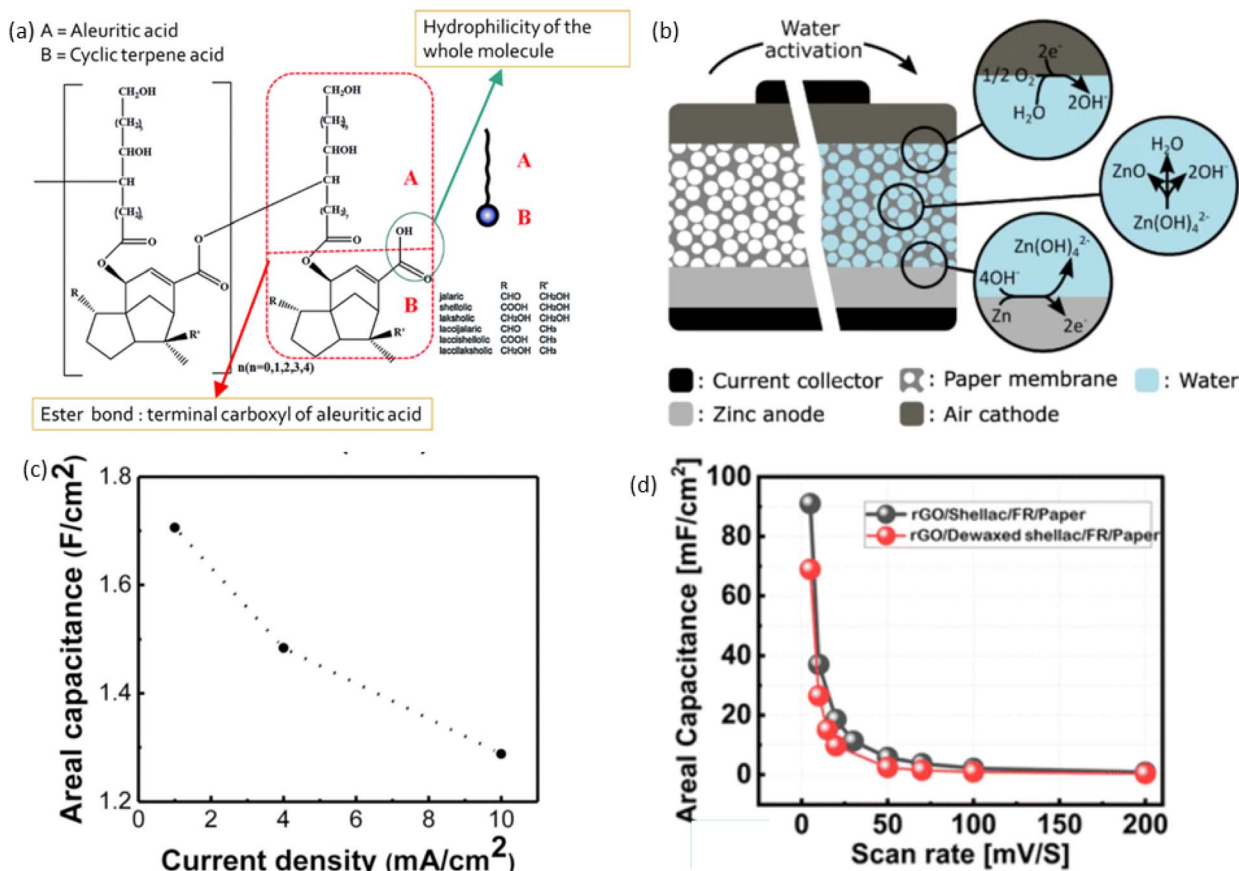


Fig. 4 (a) Chemical structure of shellac, reproduced with permission from Elsevier, ref. 153, copyright 2022 (b) shows a schematic of the water-activated battery, ref. 156, (c) graphene coated Ni foam SC, using 6 M KOH as the electrolyte, exhibited a high areal capacitance of  $1.7 F\text{ cm}^{-2}$ , reproduced with permission from Elsevier, ref. 157, copyright 2024 and (d) rGO SC developed on the dewaxed shellac paper substrate exhibited areal capacitance ranging from  $68.8 mF\text{ cm}^{-2}$  to  $0.3 mF\text{ cm}^{-2}$ , ref. 158.

natural insulating properties limit its conductivity, requiring modifications for better performance in energy storage devices.

The three main methods used to process shellac are by heat process,<sup>160</sup> solvent extraction,<sup>161</sup> and country process.<sup>162</sup> Heat process is when seedlac is melted using steam heat and pressed through a filter with hydraulic force. The filtered lac is then stretched into long sheets using a sheeting roller and fragmented into small flakes called machine-made shellac. In the solvent extraction process, seedlac is dissolved in a solvent (usually alcohol), allowing the insoluble residue to settle before filtration. The solvent is then distilled off, and the molten shellac is stretched with a sheeting roller. The solvent can be reused after rectification. Using hot alcohol produces ordinary wax-containing shellac, while cold alcohol produces dewaxed shellac since lac waxes are insoluble in cold alcohol. If decolorisation is needed, the alcoholic extract is treated with a decolourising agent before distillation. The country process is a traditional, manual method. Seedlac is placed into a long cloth bag (about 10 m long and 5–7.5 cm in diameter) and heated portion-wise in an oven with a charcoal fire. One end of the bag is kept near the oven, while the other is twisted manually. The heat and twisting pressure cause the lac resin and wax to melt and squeeze out of the bag. The molten lac is scraped off the bag's surface with a spatula and mixed with water to mitigate thermal effects. Once enough resin is collected, it is transferred to a hot water container to keep it molten. This material is then spread into a sheet and manually stretched to ensure uniform thickness and gloss. After cooling, the sheet is broken into small flakes to use.

Shellac exhibits distinct solubility characteristics, being insoluble in water, glycerin, hydrocarbon solvents, and esters, but soluble in alcohol and organic acids.<sup>154</sup> Its alkali solubility allows it to self-assemble into nanoparticles through a pH-shift method.<sup>154</sup> Studies have shown that shellac is insoluble in weak hydrogen-bonded solvents but soluble in moderate to strong hydrogen-bonded solvents.<sup>154</sup> The partial solubility of shellac in ether has been utilised to separate it into hard/pure (insoluble) and soft (soluble) resin fractions. Shellac is also soluble in acetic acid, ethyl and methyl alcohols, caustic soda, sodium carbonate, and borax solutions, with partial solubility in ethyl acetate, ether, chloroform, carbon disulfide, and acetone.<sup>153</sup> However, it remains insoluble in petroleum ether, benzene, and toluene. After extensive research, alcohol, organic acids, and ketones have been identified as the best solvents for shellac.<sup>153</sup>

Shellac is denser than water and has softening and melting temperatures ranging from 65 to 70 °C and 75 to 80 °C, respectively. When shellac is heated above its melting point for prolonged periods, it may gradually lose its fluidity and develop hard, horn-like, insoluble products, particularly after passing through the rubbery phase. This occurs because shellac contains free hydroxyl and carboxyl groups, which make it highly reactive and prone to interesterification at temperatures exceeding 70 °C.<sup>153</sup> Additionally, shellac has a thermal conductivity of 0.0024 to 0.0025 W cm<sup>-1</sup> °C<sup>-1</sup> at 30 °C, a surface resistivity ranging from 0.4 to 175 × 10<sup>13</sup> Ω cm, and an ultimate tensile strength of approximately 10 to 14 MPa at 20 °C.<sup>153</sup>

Recently, shellac has been used to fabricate EESDs, including batteries and SCs. Shellac dissolved in ethanol has been used as a binder to prepare both cathode and anode inks. The cathode ink consists of graphite flakes and polyethylene glycol, while the anode ink consists of zinc powder and polyethylene glycol. These inks are used for paper-based, water-activated metal-air electrochemical cells. Fig. 4(b) shows a schematic of the water-activated battery, which is manufactured without an electrolyte, keeping the anode and cathode separated. Water added to the system absorbs through the paper, dissolving NaCl and activating the electrochemical cell. Multiple cells can be printed on the same substrate and connected in series for higher voltages.<sup>156</sup> Shellac was used as a carbon source for graphene synthesis to fabricate graphene/nickel foam SC electrodes. The cleaned stainless steel 316 and Ni foam were dip-coated with shellac, air-dried, and the process repeated three times to ensure full graphene coverage. Direct graphene synthesis on carbon fibre fabric was difficult due to its hydrophobicity, so a thin (~60 nm) catalytic Ni layer was applied using a thermal evaporator. The coated substrates were then heated at 830 °C in a vacuum chamber for 15 minutes to form graphene. The resulting graphene coated Ni foam SC, using 6 M KOH as the electrolyte, exhibited a high areal capacitance of 1.7 F cm<sup>-2</sup> as shown in Fig. 4(c).<sup>157</sup> SC were fabricated by dip-coating shellac and dewaxed shellac onto a paper and cloth substrate, with rGO produced using laser irradiation. Laser irradiations were optimised on treated paper and cloth samples to produce high-quality rGO material. The fire retardant (FR) solution, consisting of 12.75 g Na<sub>2</sub>B<sub>4</sub>O<sub>7</sub> and 5.67 g H<sub>3</sub>BO<sub>3</sub> in 190 mL of DI water, was prepared. The FR solution was dip-coated onto both substrates and dried at 55 °C for 15 minutes to ensure complete drying. Biopolymer solutions of dewaxed shellac (DS) and shellac (S) were prepared by varying the biopolymer-to-IPA solvent ratio from 1/1 to 1/5 (w/v). The rGO SC developed on the dewaxed shellac paper substrate exhibited better areal capacitance ranging from 68.8 mF cm<sup>-2</sup> to 0.3 mF cm<sup>-2</sup> as can be seen in Fig. 4(d). In contrast, the rGO SC developed on the shellac paper substrate showed a higher areal capacitance, ranging from 91 mF cm<sup>-2</sup> to 0.7 mF cm<sup>-2</sup>.<sup>158</sup> Shellac dissolved in ethanol was used as a binder to fabricate cathode and anode inks. The cathode ink consisted of graphite, carbon black, and polyethylene glycol, while the anode ink contained zinc powder and polyethylene glycol. For the current collector, a mixture of carbon black, graphite powder, and polyethylene glycol was applied to cellulose paper to create the battery.<sup>163</sup> A fully 3D-printed disposable paper SC was fabricated using current collector ink consisting of graphite, carbon black, and shellac dissolved in ethanol and pentanol. The results showed conductivities of 260.8 ± 20.1 S m<sup>-1</sup>, 219.8 ± 21.3 S m<sup>-1</sup>, and 228.1 ± 22.6 S m<sup>-1</sup> when measured parallel, perpendicular, and at 45° to the printed lines, respectively.<sup>164</sup>

### 3.3. Polylactic acid (PLA)

PLA is one of the most ubiquitous and commercially significant biopolymers globally, with production volumes increasing from 0.2 million tons in 2015 to 0.3 million tons in 2019 and reported



to reach 2 million tons by 2035.<sup>165</sup> It is produced from lactic acid, which is obtained through the fermentation of starch found in sugarcane and corn. PLA's production reflects its growing importance and adoption in various industries due to its biodegradable nature and the sustainable production process. PLA is mostly used in packaging, agriculture, medical devices, and other applications that benefit from its environmental advantages. Also, it has demonstrated significant potential to replace conventional petrochemical-based polymers in industrial applications and to serve as a leading biopolymer in agriculture, biomedical devices, textiles, and 3D printing.<sup>166</sup> The biomedical applications of PLA date back to the 1970s, when it was initially used as sutures. In the 1980s, companies like Cargill, DuPont, and Coors Brewing began to recognise its potential, leading to increased research and development. Subsequently, PLA production was scaled up to meet the growing demands. This expansion was driven by PLA's biodegradability and its suitability for medical applications such as sutures, drug delivery systems, and tissue engineering, solidifying its status as a key material in the biomedical field.<sup>167</sup> Most of the manufactured PLA is used in packaging. Due to its biodegradability, PLA offers several end-of-life (EoL) options, including mechanical recycling, chemical recycling, landfilling, and industrial composting. Notably, compostability under aerobic conditions within 6–12 weeks. PLA's versatility in packaging stems from its ability to decompose into non-toxic by-products, making it an environmentally friendly alternative to traditional plastics. Its EoL options enhance its appeal, promoting sustainable waste management and reducing the environmental impact of packaging materials.<sup>167</sup>

PLA is a linear aliphatic thermoplastic polyester produced from renewable resources and is readily biodegradable. It serves as an environmentally friendly alternative to conventional polymers such as polyethylene (PE), polypropylene (PP), polyethylene terephthalate (PET), and polystyrene (PS).<sup>168</sup> PLA is the most extensively researched and utilised biodegradable and renewable aliphatic polyester. It is produced through the ring-opening polymerisation of lactide, with lactic acid monomers derived from the fermentation of sugar feedstocks. The fermentation process, primarily using D-glucose from corn and other biomass substrates, has significantly reduced the cost of lactic acid production compared to traditional petrochemical-derived methods.<sup>168</sup> These polymers can be produced using several techniques, including azeotropic dehydrative condensation, direct condensation polymerisation, and polymerisation through lactide formation. Azeotropic dehydrative condensation involves removing water to drive the reaction, while direct condensation polymerisation combines monomers directly. Polymerisation through lactide formation involves creating a lactide intermediate, which then undergoes ring-opening polymerisation. Each method offers distinct advantages and is selected based on the desired properties and applications of the final PLA product.<sup>169,170</sup>

Due to the asymmetric carbon atom in its molecule, lactic acid (LA) exists in two forms: L-LA and D-LA (Fig. 5(a)),<sup>166</sup> which are mirror images of each other. These forms have identical physical and chemical properties in their pure states, with

differences in how they rotate plane-polarised light: L-LA rotates light in one direction, while D-LA rotates it in the opposite direction. This chirality also affects interactions with other chiral substances, such as enzymes. PLA can be re-polymerised through chemical conversion when recycled back to lactic acid, despite having a lower maximum continuous use temperature compared to polymers like PETE.<sup>174</sup> PLA possesses good mechanical properties, such as rigidity and tensile strength, due to its linear chain structure, making it useful as a structural component in batteries and SCs, though its brittleness limits flexibility; while PLA is naturally an electrical insulator due to its non-conductive polymer backbone, it can be functionalised with conductive materials like carbon nanotubes or polymers to enhance conductivity, and its biodegradable nature offers an eco-friendly option for energy storage devices, though stabilisation is needed to prevent degradation during operation; additionally, the hydroxyl and carboxyl groups in PLA allow for chemical modifications to improve ionic conductivity and compatibility with electrolytes and other active materials.

The properties of PLA depend on its component isomers, annealing time, processing temperature, and molecular weight ( $M_w$ ). The stereochemistry and thermal history directly influence PLA crystallinity, significantly impacting its overall properties. Crystallinity refers to the amount of crystalline region in the polymer compared to its amorphous content. This characteristic affects many properties, including hardness, modulus, tensile strength, stiffness, crease resistance, and melting points. Therefore, when selecting a polymer for a specific application, its crystallinity is a crucial consideration. The physical characteristics of PLA, such as density, heat capacity, and mechanical and rheological properties, are influenced by its glass transition temperature ( $T_g$ ). For amorphous PLA,  $T_g$  is crucial since polymer chain mobility changes significantly at and above this temperature. In semicrystalline PLA, both  $T_g$  and melting temperature ( $T_m$ ) are important for predicting behaviour. The melting enthalpy for enantiopure PLA with 100% crystallinity ( $\Delta H_m^\circ$ ) is typically  $93\text{ J g}^{-1}$ , though values up to  $148\text{ J g}^{-1}$  have been reported.  $T_m$  and crystallinity degree depend on molar mass, thermal history, and polymer purity. The density of amorphous and crystalline poly(L-lactic acid) (PLLA) is reported as  $1.248\text{ g cm}^{-3}$  and  $1.290\text{ g cm}^{-3}$ , respectively. Solid PLA has densities of  $1.36\text{ g cm}^{-3}$  for L-lactide,  $1.33\text{ g cm}^{-3}$  for meso-lactide,  $1.36\text{ g cm}^{-3}$  for crystalline PLA, and  $1.25\text{ g cm}^{-3}$  for amorphous PLA. In food packaging, the ability of PLA (polylactic acid) to block gases, water vapor, and aroma molecules is very important. Additionally, PLA's transparency is key for dyeing textiles and packaging. Hutchinson and colleagues studied the optical properties of PLA with different amounts of stereoisomers using a technique called ellipsometry. They also created an equation to calculate the refractive index of PLA with different stereoisomer proportions (L-content) across wavelengths from 300 to 1300 nm using Cauchy coefficients. PLA products generally dissolve in solvents like dioxane, acetonitrile, chloroform, methylene chloride, 1,1,2-trichloroethane, and dichloroacetic acid. PLA partially dissolves in ethyl benzene, toluene, acetone, and tetrahydrofuran when cold but dissolves more easily in these solvents when heated to boiling



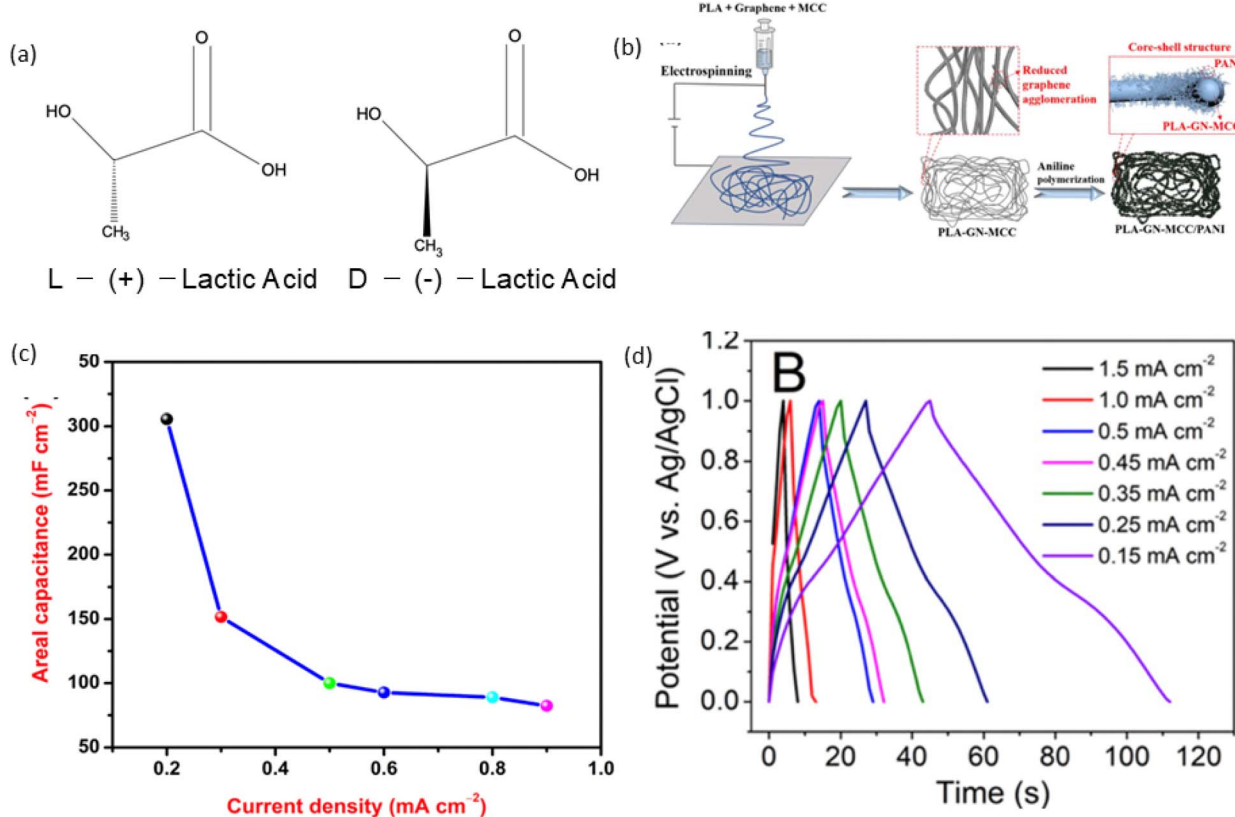


Fig. 5 (a) Enantiomeric forms of lactic acid,<sup>166</sup> (b) illustrates the preparation process of the PLA-GN-MCC/PANI electrode, reproduced with permission from Elsevier, ref. 171, copyright 2023 (c) the PLA-based SC showed an areal capacitance of  $303.5 \text{ mF cm}^{-2}$  at a current density of  $0.2 \text{ mA cm}^{-2}$ , reproduced with permission from Elsevier, ref. 172, copyright 2023 and (d) a PLA-based free-standing, binder-free film electrode achieved a high areal capacitance of  $10 \text{ mF cm}^{-2}$  at a current density of  $0.15 \text{ mA cm}^{-2}$ , reprinted with permission from American Chemical Society, ref. 173, copyright 2021.

temperatures. Lactic acid-based polymers do not dissolve in water, alcohols, or in hydrocarbons. PLA primarily breaks down through hydrolysis, a process that happens over several months when exposed to moisture. This degradation occurs in two stages. First, the ester groups in the PLA chains break apart randomly, lowering the molecular weight ( $M_w$ ). In the second stage, the molecular weight continues to decrease until the lactic acid and low  $M_w$  oligomers are naturally metabolised by microorganisms into carbon dioxide and water.<sup>166</sup> Some of the advantages and disadvantages of PLA are shown in Table 4.

In recent years, PLA has been widely used in enhancing the electrochemical capabilities of EESDs by advancing electrode materials. PLA/halloysite nano-clay has been utilised as an electrode material for SC.<sup>175</sup> PLA combined with poly(vinylidene fluoride-*co*-hexafluoropropylene) (PVDF-HFP) has been used to fabricate gel polymer electrolytes.<sup>176</sup> Additionally, PLA has served as a substrate in the electrospinning of PLA/graphene (GN)-microcrystalline cellulose (MCC)/polyaniline (PANI) nanofibers to create flexible SC electrodes. Fig. 5(b) illustrates the preparation process of the PLA-GN-MCC/PANI electrode. The PLA-GN-MCC material was produced through electrospinning a solution mixture of PLA, GN, and MCC. The incorporation of MCC helps to reduce the stacking of GN sheets. The PLA-GN-MCC/PANI electrode, featuring a coated structure, was

created by polymerizing aniline onto the PLA-GN-MCC substrate, the resulting SC fabricated with PLA-GN-MCC/PANI electrode and  $1 \text{ M H}_2\text{SO}_4$  electrolyte showed the specific capacitance of  $16.54 \text{ F g}^{-1}$  ( $221.64 \text{ mF cm}^{-2}$ ) at a current density of  $0.05 \text{ A g}^{-1}$ .<sup>171</sup> PLA-1 wt% poly(4-styrene sulfonate) (PSS) membranes have shown high performance, PLA was prepared by dissolving 4 g of PLA in chloroform and stirring for 3 hours. Separately, a solution of PSS was created by dissolving PSS in chloroform with two drops of concentrated HCl. The desired amount of PSS was then added to the PLA solution, forming a homogeneous mixture. This solution was cast onto a clean glass frame and allowed to dry completely at room temperature before the membrane was peeled off. The SC showed an areal capacitance of  $303.5 \text{ mF cm}^{-2}$  at a current density of  $0.2 \text{ mA cm}^{-2}$  as shown in Fig. 5(c), and an energy density of  $15.8 \text{ } \mu\text{W h cm}^{-2}$  at a power density of  $243.9 \text{ } \mu\text{W cm}^{-2}$ .<sup>172</sup> Flexible and conductive poly(lactic acid)/graphite composite films with a high mass percentage ( $\sim 64\%$ ) of conductive graphitic material have also been developed. PLA was dissolved in DCM with stirring at a mass-to-volume ratio of 1 : 10. mPEG-750 was added under continuous stirring at a concentration of 40% by mass relative to PLA, followed by the addition of graphite powder at a mass ratio of 7 : 3 (graphite to PLA). It resulted in a suspension suitable for film casting. The films were left to dry for 5–10



Table 4 Advantages and disadvantages of PLA

Advantages	Disadvantages
PLA is made from renewable sources like corn, wheat, and rice. It is biodegradable, recyclable, and compostable, and its production absorbs CO <sub>2</sub>	PLA is very brittle, with a break elongation of less than 10%. This limits its use in modern applications such as stretchable EESDs
The primary product of PLA degradation, lactic acid, is non-toxic and metabolised by organisms	PLA degrades naturally through hydrolysis, with its rate influenced by factors like crystallinity and molecular weight. Slow degradation results in long device lifetimes but poses issues with disposal
PLA has superior thermal processability compared to other biopolymers, enabling methods such as injection moulding, film extrusion, fibre spinning Compared to petroleum-based polymers, PLA production consumes 25–55% less energy	PLA's water contact angle of approximately 80° indicates its hydrophobic nature. This property results in low cell affinity and can trigger inflammatory responses when in direct contact with biological fluids The chemical inertness of PLA complicates both surface functionalisation and bulk modification process

minutes before being peeled off the glass. The SC GCD results (Fig. 5(d)) showed a free-standing, binder-free film electrode achieved a high areal capacitance of 10 mF cm<sup>-2</sup> at a current density of 0.15 mA cm<sup>-2</sup>.<sup>173</sup> Polyaniline (PANI) and graphene/polyaniline (Gr/PANI) composites have been prepared by *in situ* chemical polymerisation. As a biodegradable polymer, PLA has been used as an adhesive for electrode materials in SC, replacing traditional polyvinylidene fluoride (PVDF) adhesives.<sup>177</sup> PLA thin films, including poly(vinyl alcohol) (PVA), zinc oxide (ZnO), and tungsten oxide (WO<sub>3</sub>), have been prepared to create simple, low-cost, and biocompatible photo-induced K-ion-based power cells.<sup>178</sup> Additive manufactured SC have been derived from recycled PLA feedstock. Waste PLA recovered from coffee pods was melt-compounded with a plasticiser (polyethylene glycol) and a conductive filler (carbon black) to fabricate high-voltage, low-cost aqueous SC electrodes.<sup>179</sup> Also, PLA was infused with a mixture of ethyl methyl carbonate, propylene carbonate, and LiClO<sub>4</sub> to achieve an ionic conductivity of 0.085 mS cm<sup>-1</sup>, comparable to polymer and hybrid electrolytes. Various electrically conductive materials (Super P, graphene, MWCNT) and active materials (lithium manganese oxide, lithium titanate) were blended into PLA to study the relationships among filler loading, charge storage capacity, electrical conductivity, and printability for fully 3D-printed LIBs.<sup>180</sup>

### 3.4. Chitin

Chitin, the second most abundant biopolymer after cellulose, is a natural polysaccharide found in various organisms, including sponges, mollusks, nematodes, arthropods, and fungi.<sup>181</sup> It forms a significant part of their body mass, ranging from 3 to 40%.<sup>182</sup> Chitosan, *N*-acetyl glucosamine (GlcNAc), and chitooligosaccharides (COS) are the leading derivatives of chitin.<sup>183</sup> Chitin has a crystalline morphology and an interface that interacts more strongly with proteins. It is extracted through mechanical, chemical, chemo-mechanical, and eco-friendly biological methods.<sup>184</sup> The intrinsic antibacterial, nontoxic, and biodegradable properties and facility of processibility of chitin make it a potential alternative for developing energy and environmental applications. Its nontoxicity and good biocompatibility make it a promising candidate for various industries, including agriculture, food, textiles, and bioengineering. This well-established biopolymer found extensively in the

extracellular matrix of lower plant fungi, crustaceans like shrimp and crabs, insects, and fungi's cell walls. Numerous studies reported the presence of chitin in crustacean shells, melolontha melolontha, orthoptera species, insect cuticles, wings of cockroaches, grasshopper species, medicinal fungus, larvae and adult of Colorado potato beetle aquatic invertebrates, bat guano, resting eggs of *Daphnia longispina*, spider species, *Daphnia magna* resting eggs, and lastly, in green algae and fungi cell walls.<sup>181</sup> Chitin can also be found in waste flows such as silkworm larvae, seafood by-products, or processed food waste from insect biomass. Its structure and properties vary with its source.<sup>182</sup>

The extraction of chitin involves two main steps: demineralisation and deproteinization. Chitin extraction can be performed using chemical or biological methods.<sup>184</sup> Chemical extraction includes initially, HCl removing mineral constituents like calcium carbonate and calcium phosphate. Stirring with 3% sodium hypochlorite for 10 minutes is efficient for demineralisation. Other acids such as HNO<sub>3</sub> and H<sub>2</sub>SO<sub>4</sub> are also used for deproteinization. After strong acids are used, demineralisation is performed using NaOH. To prevent deacetylation and property degradation, deproteinization is preferably carried out at ambient temperature in a stirred reactor, reducing process duration. Finally, acetone or an organic solvent mixture is used for decolourisation.<sup>184</sup> The biological methods, such as using lactic acid-producing bacteria for demineralisation and specific bacteria like *Pseudomonas aeruginosa* and *Bacillus subtilis* for deproteinization by fermentation. Chemical extraction offers benefits such as shorter processing time, a high degree of deacetylation, industrial viability, and complete removal of organic salts. However, it is not environmentally friendly. In contrast, biological methods are environmentally safe and produce high-quality products but takes prolonged processing time.<sup>184</sup>

Chitin is a long polysaccharide composed of two monomer units, namely *N*-acetyl-2-amino-2-deoxy-*D*-glucose (*N*-acetyl-*D*-glucosamine) and (2-amino-2-deoxy-*D*-glucose) *D*-glucosamine units which are linked by 1-4- $\beta$ -glycosidic bonds as shown in Fig. 6(a). A typical monomer has two hydroxyl groups: primary hydroxyl at C-6, secondary hydroxyl at C-3, and amino groups or *N*-acetyl group (at C-2) positions.<sup>185</sup> The *N*-acetyl group can form linear inter and intramolecular hydrogen bonds, resulting in



higher crystallinity, molecular weight increase, and water insolubility. The biopolymer is generally considered as chitin only if *N*-acetyl-2-amino-2-deoxy-D-glucose (*N*-acetyl-D-glucosamine) content is less than 50. The structure of chitin is studied mainly from its three different source groups: aquatic invertebrates, insects, and fungi.<sup>181</sup> According to the studies, chitin is exhibited primarily on three polymorphs:  $\alpha$ -chitin,  $\beta$ -chitin, and  $\gamma$ -chitin. Each polymorph, from the main isomorph  $\alpha$ -chitin present in the exoskeletons of crustaceans and mollusks to the unique  $\beta$ -chitin found in squid pens and the rare  $\gamma$ -chitin existing in the cocoon fibres of *Ptinus* beetles, is a testament to the diversity of nature. The main difference between these polymorphs is the stacking arrangement of the polymeric chitin chains.  $\alpha$ -Chitin and  $\beta$ -chitin contain polymeric chitin chains stacked in anti-parallel and parallel configurations.<sup>188</sup> At the same time,  $\gamma$ -chitin consists of both anti-parallel and parallel arrangements of chitin chains. This difference in stacking arrangement creates different degrees of H-bonding interactions from the amide functional groups between the polymeric chains and thus exhibits different properties for the three polymorphs.<sup>189</sup> Chitin is similar to cellulose, but the main difference is that acetamido residues have replaced the C2 hydroxyl groups. Because of their structural features, these biomaterials exhibit unique physical, chemical, mechanical, and optical properties, contributing to low density, high porosity, renewability, and, most importantly, environmental friendliness. Chitin exhibits high tensile strength and rigidity due to its crystalline structure and hydrogen bonding, making it suitable for providing structural integrity in EESDs, while its biocompatibility and biodegradability render it an

environmentally friendly option, although modifications may be needed for enhanced durability; additionally, its amine and hydroxyl functional groups enable chemical modifications to improve conductivity and ionic transport properties, and its hydrophilic nature facilitates interactions with electrolyte ions, further enhancing its electrochemical performance in batteries and SC.

Due to its unique structure, high porosity, lightweight nature, and effective interaction with various polymers, it is highly suitable for developing electrode and electrolyte materials in batteries and SC. Electrically conducting elements will combine with chitin to develop electrode materials using blending, vacuum filtration, *in situ* polymerisation, electrodeposition, *etc.* Due to the higher surface area of carbon-derived biomass, it can enhance the double-layer capacitance. Moreover, studies show that the presence of heteroatoms such as nitrogen, sulphur, oxygen, boron, and phosphorous *etc.* in biomass-derived carbon can increase the wettability of carbon and pseudo capacitance. Therefore, the presence of heteroatoms in carbon-derived chitin can improve the electrical conductivity and the overall specific capacitance of the energy storage device. The mechanical stability and enhanced electrical conductivity make it suitable for flexible energy storage devices. Nano chitin is the basic building block of chitin. It assembles semicrystalline chitin nanofibrils that show highly oriented nanocrystals embedded in a fluid matrix. Single nanofibrils are packed into highly positioned microfibrils or fibril bundles held together by van der Waals forces and hydrogen bonding (H-bonding).<sup>182</sup> Chemically, it is narrowed by a covering of proteins and is gathered into elongated fibrils

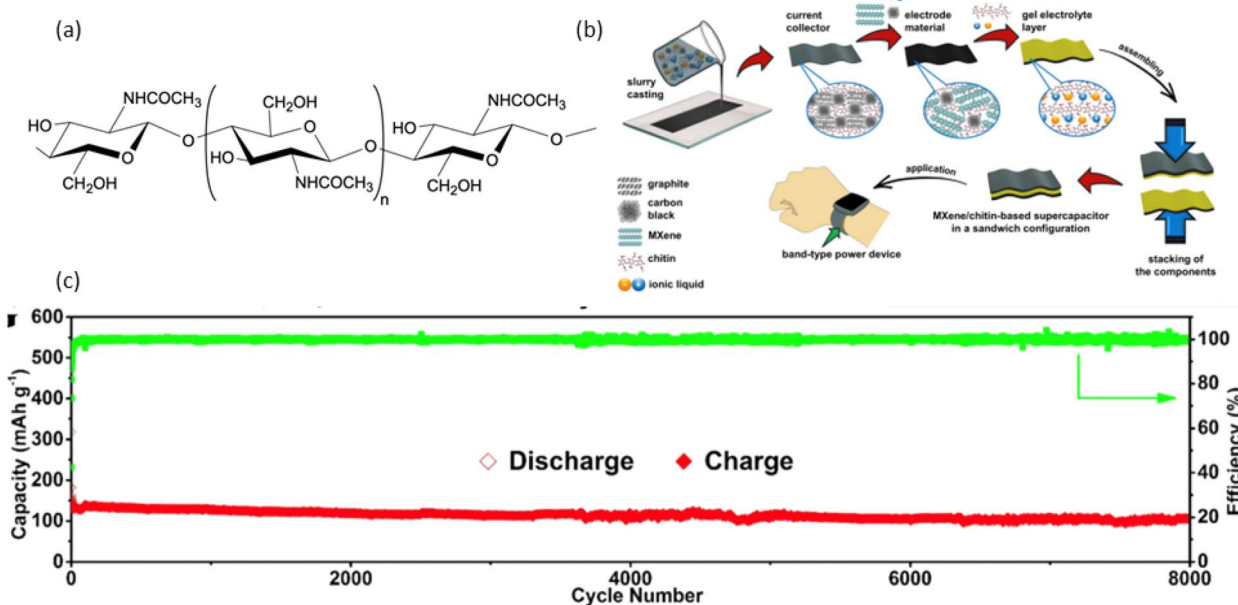


Fig. 6 (a) Chemical structure of chitin,<sup>185</sup> (b) a solid-state chitin-based current collector, electrode material, and gel electrolyte SC fabrication, reproduced with permission from John Wiley & Sons, ref. 186, copyright 2023 (c) direct pyrolysis of chitin used as electrode material for sodium-ion battery showed impressive lifespan of over 8000 cycles, with a coulombic efficiency nearing 100%, reproduced with permission from Elsevier, ref. 187, copyright 2018.



embedded in a mineral protein matrix in the exoskeleton of arthropods. Among other natural nanopolysaccharides, it has characteristics of rodlike structure, nanometre lateral dimension, crystallinity, and nitrogen content.<sup>182</sup> There are two types of nano chitin nanofibers and chitin nanocrystal. As like chitin, its properties depend upon its source, extraction, and modification methods.

Processed nano chitin were also used in the development of battery elements. Recent development of electrode materials using chitin, electrolytes were also reported for both SC and batteries by combining chitin with polymer monomer using processes like grafting, inorganic fillers, and blending.<sup>185</sup> Hydrophilic functional groups in chitin, such as  $-\text{OH}$ ,  $-\text{COOH}$ ,  $-\text{NH}_2$ , and  $\text{CONH}_2$ , provide them with excellent wetting capabilities toward polar solvents, making them suitable for electrolyte development.<sup>190</sup> The modified chitin acquires higher conductivity by reducing the crystallinity of chitin in its form. A chitin-based current collector, electrode material, and gel electrolyte for a solid-state MXene/chitin-based SC were reported (Fig. 6(b)). Gel electrolyte achieved an ionic conductivity of  $8.5 \pm 0.4 \text{ mS cm}^{-1}$  using chitin and ionic liquids, the SC can achieve a maximum energy density of  $3.55 \text{ W h kg}^{-1}$  at a power density of  $81.1 \text{ W kg}^{-1}$ .<sup>186</sup> Like SC, chitin-based batteries are a growing technology in energy storage. A sodium ion battery electrode was fabricated using N-doped amorphous carbon nanofibers were synthesised through a simple direct pyrolysis of pure chitin. First, a chitin sample was preheated from room temperature to  $300 \text{ }^\circ\text{C}$  in an argon atmosphere for 1.5 hours at a heating rate of  $1 \text{ }^\circ\text{C min}^{-1}$  to stabilize the nanostructure. Next, the prepared precursor was carbonized at the designated temperature for 2 hours in a tube furnace under argon flow at a heating rate of  $5 \text{ }^\circ\text{C min}^{-1}$ . The carbonization temperatures were set at  $500$ ,  $600$ ,  $700$ ,  $800$ , and  $900 \text{ }^\circ\text{C}$ , resulting in

carbonized chitin. The electrode materials demonstrated a high reversible specific capacity of  $320.6 \text{ mA h g}^{-1}$ , an energy density of  $192 \text{ W h kg}^{-1}$ , excellent rate capability, and an impressive lifespan of over 8000 cycles, with a coulombic efficiency nearing 100% as shown in Fig. 6(c).<sup>187</sup> The major developments in chitin-based energy storage devices were the development of chitin-derived carbon, chitin-based electrolytes, chitin-based binders, and nano chitin. Some of the recent chitin-based materials development for batteries and SCs are shown in Tables 5,<sup>187,191-195</sup> and 6,<sup>186,196-200</sup> respectively.

### 3.5. Chitosan

Chitosan is a modified polycationic biopolymer formed by the partial deacetylation of chitin. It is a nitrogenous, rigid, white, and inelastic polysaccharide. Chitin, a polymer of *N*-acetyl-D-glucosamine, is deacetylated to create  $\beta$ -1,4-D-glucosamine, also known as chitosan, which lacks the acetyl functional group.<sup>201</sup> It has been found that chitosan is safe, biodegradable, and biocompatible. Despite being insoluble in water, chitosan is soluble in acidic solvents such as diluted hydrochloric, formic, and acetic acids.<sup>202</sup> Chitosan exhibits stronger chemical and biological reactivity than chitin because it contains free primary amino groups that spread across its molecular chain. Therefore, the industrial applications of chitosan as antimicrobials, biomedical materials, food additives, separators, sewage disposal, agricultural materials are receiving attention globally.<sup>203</sup> Chitosan is particularly well-known in the packaging industry because of its strong film forming characteristics. Chitosan is utilised in the development of antithrombogenic materials for gene carriers, controlled release, drug encapsulation, enzyme, and cell immobilisation, and more. The biodegradability, antimicrobial activity, hydrophilicity, and presence

Table 5 Chitin-based materials for batteries

Type of battery	Battery element produced from chitin	Electrochemical performance	Ref.
Sodium-ion batteries (SIBs)	Anode material: nitrogen-doped amorphous carbon nanofibers	$115 \text{ mA h g}^{-1}$ when constructed by combining a Prussian blue cathode while retaining 90% of the capacity after 200 cycles	187
Sodium sulphur batteries	Cathode material: nitrogen self-doped hierarchical meso- and microporous carbon (NSPC) is synthesized from chitin and used to confine sulfur ( $\text{S} \subset \text{NSPC}$ ) Separator: chitinnanofiber membrane (CNM) loaded with sodium dihydrogen citrate separator	Reversible capacities of $1207 \text{ mA h g}^{-1}$ at $0.1\text{C}$ and $891 \text{ mA h g}^{-1}$ at $2\text{C}$	191
Li/Na-ion batteries		Discharge capacity of $157 \text{ mA h g}^{-1}$	192
Lithium-ion battery	Separator: fluorinated polymer-coated cyanoethyl-chitin nanofiber composite separators	Better capacity retention of 90.2% after 100 cycles at $1\text{C}$	193
Zinc-ion batteries	Electrolyte: gel polymer electrolyte from chitin nanofibrils	Provides $41 \text{ mA h g}^{-1}$ after 600 cycles at $100 \text{ mA g}^{-1}$	194
Aqueous battery	Electrolyte: carboxymethyl chitin (CMChit) as a solid polymer electrolyte (SPE)	Ionic conductivity in the order of $10^{-4} \text{ S cm}^{-1}$ and electrochemical stability was up to 2.93 V	195



Table 6 Chitin-based materials for supercapacitor

Electrode material	Electrolyte	Specific capacitance	Power density (energy density)	Cycling stability	Ref.
Chitin-based porous carbon	PVA/KOH	69.6 F g <sup>-1</sup> (0.25 A g <sup>-1</sup> )	-(9.67 W h kg <sup>-1</sup> )	90.2% (10 000)	196
Chitin-based porous carbon	6 M KOH	221 F g <sup>-1</sup> (0.5 A g <sup>-1</sup> )	0.19 kW kg <sup>-1</sup> (15.41 W h kg <sup>-1</sup> )	96% under 5000 long cycles	197
MXene carbon black chitin	Chitin/ionic liquid hydrogel	113–115 F g <sup>-1</sup>	81.1 W kg <sup>-1</sup> (3.55 W h kg <sup>-1</sup> )	85% under 10 000 long cycles	186
Zeolitic imidazole assisted N-doped hierarchical porous carbon from chitin nanofibers	6 M KOH	182.5 F g <sup>-1</sup> @ 0.2 A g <sup>-1</sup>	50 W kg <sup>-1</sup> (4.46 W h kg <sup>-1</sup> )	90% after 5000 cycles	198
N,O co-doped activated carbon from chitin	1 M H <sub>2</sub> SO <sub>4</sub> and 6 M KOH; PVA (PVA)/H <sub>2</sub> SO <sub>4</sub>	204 F g <sup>-1</sup> @ 0.5 A g <sup>-1</sup>	9.9 W kg <sup>-1</sup> (4.53 W h kg <sup>-1</sup> )	100% after 25 000 cycles	199
N-doped nanofibrous chitin microspheres	EMIM TFSI	113 @ 1 mV s <sup>-1</sup>	300 W kg <sup>-1</sup> (58.7 W h kg <sup>-1</sup> )	96% after 10 000 cycles	200

of polar groups that can create secondary interactions with other polymers are all advantages of chitosan-based products. Processing chitosan into a fibre, film, sponge, bead, gel, or solution is simple. The formation of electrostatic compounds and/or multilayer structures is also made possible by its cationic charge. The availability of free  $-\text{NH}_2$  groups within chitosan chains enables certain changes to be made under mild settings. Chitosan can also be combined with natural or synthetic polymers.<sup>201</sup> Additionally, chitosan can be applied for water treatment, and solar cell applications due to its unique properties like ease of charge transfer and large electrons density.<sup>204</sup> Chitosan has become a viable alternative for the creation of electrode and electrolyte materials in EESDs.

Chitosan is produced from chitin extracted from crustacean shells, insect exoskeletons, and the cell walls of numerous fungi. Shrimp and crabs are the most often mentioned sources of raw materials used to prepare chitosan. While other species including lobster, crayfish, and oyster have also been used. Even though chitosan is found in a broad variety of species and that its concentration varies among them, crustacean by-products with at least 20% chitin, such lobster cephalothorax, are viable sources for the commercial synthesis of chitosan. The utilisation of 40–50% by weight of the total mass of crustaceans for human consumption ends up as waste, and the majority of this waste is discarded into the sea and causes major pollution in coastal areas, which explains the economic and environmental benefits of using crustacean sources for chitosan preparation.<sup>205</sup> However, chitosan is becoming more widely available as a by-product of silk cocoon farming, protein extraction from insects for food/animal feed, and fungal fermentation. The annual production of chitosan from crustaceans is estimated to be between 1012 and 1014 tonnes, and the global market for chitin and its derivatives was valued at US\$2900 million in 2017. This growth was achieved at a Compounded Annual Growth Rate (CAGR) of 14.8%. By 2024, it was predicted to reach US\$63 billion.<sup>206</sup> Many companies are at the forefront of the industry, producing a wide range of products for food, drug, medical, textile, and waste treatment using chitosan sourced from

shrimp shells, which accounts for nearly 80% of the market. These companies include Chinova Bioworks, Heppe Medical Chitosan GmbH, Golden-Shell Biochemical, and G. T. C. Bio-corporation.<sup>207</sup>

Chitosan is a polymer composed of both *D*- and *N*-acetyl *D*-glucosamine units as shown in Fig. 7(a). Chitosan is a copolymer made up of *D*-glucosamine and *N*-acetylglucosamine linked by  $\beta$ -1,4-glycosidic linkages. Three functional groups are present in chitosan: a primary and secondary hydroxyl group at locations C2, C3, and C6, as well as an amino group. It is the presence of amino groups that differentiate chitosan from chitin. It is feasible to undertake chemical modification on chitosan to improve its chemical and physical characteristics since it has a significant number of hydroxyl ( $-\text{OH}$ ) and amino ( $-\text{NH}_2$ ) groups with chemical activity. Once the amino groups in chitosan are protonated, they generate a polycation that may then form ionic complexes with a wide range of natural or synthetic anionic species, including DNA, lipids, proteins, and some negatively charged synthetic polymers like poly(acrylic acid). In fact, chitosan is the only positively charged polysaccharide that occurs naturally.<sup>212</sup> The development of H-bonds networks in the solid state is the basis for understanding of their fibre and film-forming properties. The characteristics of chitosan are clearly determined not only by its chemical structure, but also by its molecular conformation and packing arrangement. Chitosan has a molecular structure comparable to cellulose and chitin.<sup>208</sup> Chitosan is ideally suited for application in flexible and lightweight energy storage devices due to its unique structure, high porosity, lightweight nature, and efficient interaction with different polymers. Chitosan has shown great promise in the field of SC as an electrode and electrolyte material for a variety of applications.<sup>190</sup> Chitosan demonstrates good mechanical strength and flexibility from its partially crystalline structure and hydrogen bonding, enabling it to maintain structural integrity in energy storage applications; its biocompatibility and biodegradability make it an environmentally friendly choice, although it may need modifications to ensure stability during operation. Furthermore, the amino and

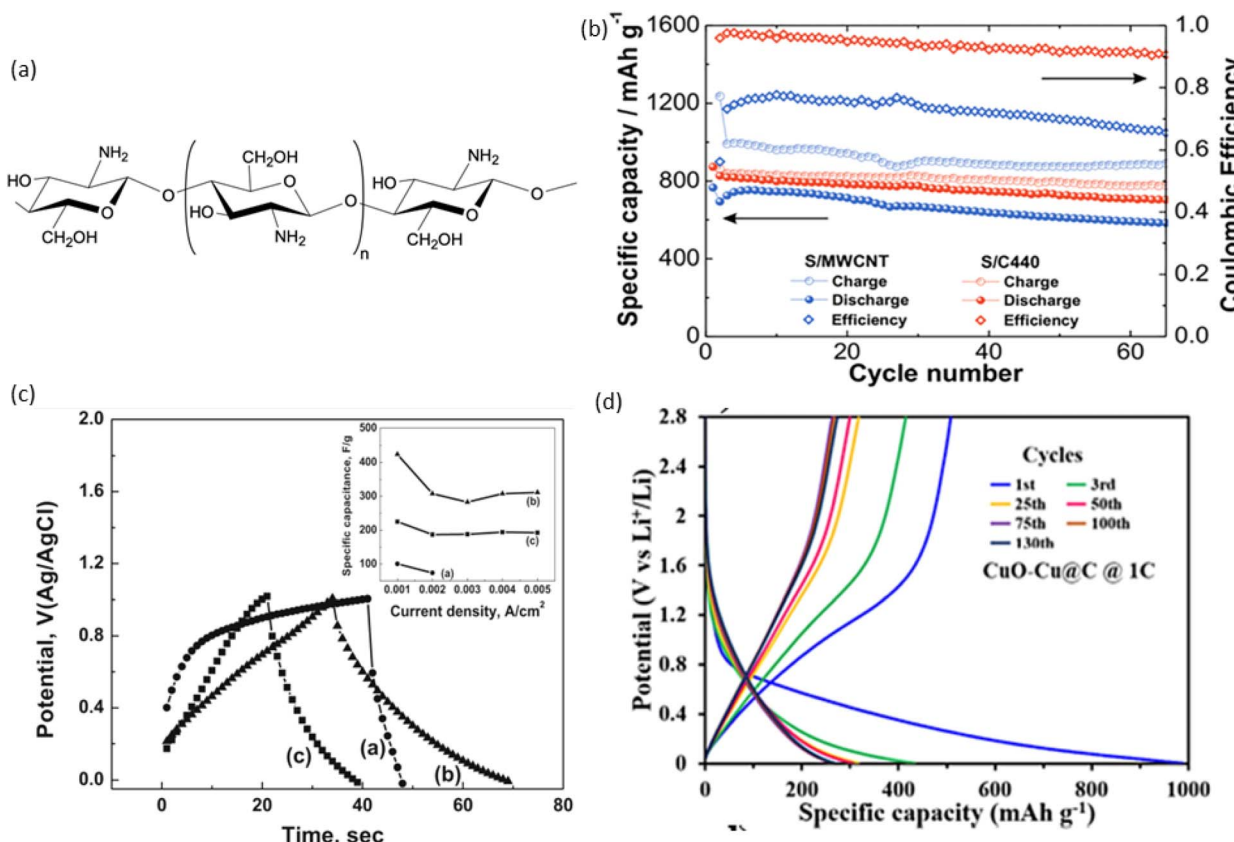


Fig. 7 (a) Chemical structure of Chitosan,<sup>208</sup> (b) the average coulombic efficiency of S/chitin heated at 440 °C was about 92%, significantly higher than that of S/MWCNT, reproduced with permission from Elsevier, ref. 209, copyright 2020 (c) MnO<sub>2</sub>-chitin (low Mw) achieved the highest specific capacitance of 424 F g<sup>-1</sup> at a current density of 1 mA cm<sup>-2</sup>, reproduced with permission from Elsevier, ref. 210, copyright 2014 and (d) the fabricated Li-ion batteries demonstrated a specific capacity of 988 mA h g<sup>-1</sup> during the initial cycle and a 265 mA h g<sup>-1</sup> even after 130 cycles at 1C, reproduced with permission from Elsevier, ref. 211, copyright 2024.

hydroxyl groups present in chitosan allow for chemical functionalisation, which can enhance its electrical conductivity and ionic transport properties, while its hydrophilic nature promotes interactions with electrolyte ions, thereby improving overall electrochemical performance in devices like batteries and SC.

Chitosan preparation is divided into two basic categories: chemical and biological processes. Chemical processes are widely employed for commercial chitosan preparation since they are cost-effective and suitable for large scale manufacturing.<sup>201</sup> When selecting an appropriate method for chitosan production, it is crucial to prioritise those that produce chitosan with higher bioactivities, as indicated by lower degrees of acetylation (DA) and MW. The chemical preparation of chitosan typically involves three main stages: demineralisation, deproteinisation, and deacetylation. During demineralisation, calcium carbonate (CaCO<sub>3</sub>) is removed from the shell using hydrochloric acid. Deproteinisation is the process of removing proteins and other organic components from the shell by treating it with a hot alkaline solution, such as sodium hydroxide (NaOH), at temperatures ranging from 65 to 100 °C for 0.5 to 12 hours. Finally, chitin is deacetylated into chitosan using heated alkaline solution, such as NaOH, at

a concentration of 40% to 50% (ref. 205) + enzymatic and fermentation procedures are classified as biological ways for producing chitosan from crustacean by-products. Enzymatic procedures use the same demineralisation mechanism as chemical approaches. However, this approach uses enzymes to carry out the deproteinization and deacetylation processes at lower temperatures, typically between 25 and 59 °C, in place of an alkaline and high reaction temperature. Despite the milder reaction conditions, enzymatic techniques have significant limits as compared to chemical methods, mainly due to greater operational costs, especially on an industrial scale. Deproteinization and deacetylation enzymes are considerably more expensive than chemical bases. Furthermore, different enzymes are required for each stage in a single manufacturing process. Enzymatic techniques are also less effective since they cannot entirely remove the final 10% of proteins during deproteinization and obtain a lower degree of deacetylation compared to chemical methods. To address the high cost of enzymes, fermentation methods have been developed as an alternative. Microbes can rapidly multiply and secrete enzymes in reactors under optimised conditions, thereby reducing enzyme costs. However, to overcome reaction inefficiency, a cycle of chemical reactions is needed to refine the product after enzymatic



reactions. This highlights the advantages of chemical methods for chitosan preparation over biological methods. Chemical processes are simpler, quicker, and produce chitosan with stronger bioactivities due to lower MW and higher degrees of deacetylation. In contrast, biological methods, despite milder reaction conditions, require hazardous microbes, specialised equipment, complex post-fermentation purification, and an additional chemical processing cycle to achieve optimal chitosan quality. However, chemical methods have their drawbacks, such as the use of toxic or corrosive chemicals like HCl and NaOH, which can produce significant pollutants if not properly managed. Considering these actors, unconventional chemical methods using KOH instead of NaOH, enhanced by microwave or ultrasound, may offer more advantages than biological methods.<sup>205</sup>

Chitosan nanoparticles (CSNP) exhibit the combined characteristics of chitosan with the distinctive features of nanoparticles, such as surface and interface effects, small size, and quantum size effects. Several approaches have been discovered for the synthesis of CSNP since Ohya and colleagues<sup>213</sup> first disclosed them in 1994 for the administration of anticancer drugs intravenously. Ionotropic gelation, microemulsion, emulsification solvent diffusion, polyelectrolyte complex, and reverse micellar approach are the five main methods of preparations of CSNP. The most popular among them are ionotropic gelation and polyelectrolyte complexes, which are simple and do not need significant shear pressures or organic solvents. The electrospinning method, which can produce fibres from micrometres to nanometres in size, is an efficient way to make chitosan nanofibers, which are solid particles with diameters ranging from 1 to 1000 nm. Solvents such as trifluoroacetic acid and acetic acid are particularly useful in this procedure. Chitosan nanoparticles are natural materials with excellent antimicrobial, biological and physicochemical properties making them environmentally friendly and safe for human use. Chitosan nanoparticles can be used in a variety of ways due to their unique features.<sup>214</sup> With a strong permeability and retention impact, chitosan-based nanoparticles can stop the development of tumour cells by causing apoptosis. Chitosan has been widely employed in dentistry, haemodialysis, gene delivery, and drug delivery as a nano-sized carrier to target tumour tissue while slightly affecting areas of normal tissue. Chitosan is suggested as a superior antibacterial nanomaterial for wound dressings.<sup>215</sup> The CSNP can be used to create customised electrodes for energy storage, SC, and biosensor applications by increasing the electrochemical characteristics.<sup>204</sup>

Recent works has explored the use of nano chitosan and nickel oxide nanoparticles to fabricate novel nanohybrid membranes for various applications including SCs and energy storage.<sup>204</sup> Chitosan was converted into nitrogen-rich biochars *via* pyrolysis at mild conditions ranging from 284 °C to 540 °C, promoting energy-efficient and low CF synthesis. Chitosan samples were heated at 10 °C min<sup>-1</sup> to 284 °C, 440 °C (C440), or 540 °C, then held for 1 hour. The resulting biochars were ball-milled with 60 wt% sulphur (S) for 30 minutes. Nitrogen-doped biochars (C284, C440, C540) were tested as sulphur hosts in Li-S batteries, with S/C440 showing an average

discharge capacity improvement of 100 mA h g<sup>-1</sup> compared to S/MWCNT. The average coulombic efficiency of S/C440 was about 92%, significantly higher than that of S/MWCNT as shown in Fig. 7(b).<sup>209</sup> Using a solution casting method, chitosan combined with LiCO<sub>2</sub>CH<sub>3</sub> and glycerol to fabricate polymer electrolytes showed high specific capacitance, energy density, and power density of 132.8 F g<sup>-1</sup>, 18.4 W h kg<sup>-1</sup>, and 2591 W kg<sup>-1</sup>, respectively.<sup>216</sup> MnO<sub>2</sub>-chitosan hybrid nanocomposite films synthesised by one-step cathodic electrodeposition on a nickel foam substrate. Two chitosan (CH) raw materials, with molecular weights of 300 000 (high) and 25 000 (low) kDa and a degree of deacetylation (DA) over 85%, were used to deposit MnO<sub>2</sub>-CH thin films. The films were cathodically deposited at -0.1 V *vs.* Ag/AgCl (KCl saturated) on nickel foam from a 0.02 M KMnO<sub>4</sub> solution, with or without 0.2 g L<sup>-1</sup> chitosan in 1% acetic acid. The film mass was controlled by adjusting the total charge during deposition, confirmed by a six-digit microbalance, MnO<sub>2</sub>-CH (low Mw) (Fig. 7(c)) achieved the highest specific capacitance of 424 F g<sup>-1</sup> at a current density of 1 mA cm<sup>-2</sup>.<sup>210</sup> A novel chitosan-induced self-assembly strategy was used to construct MXene into flexible Ti<sub>3</sub>C<sub>2</sub>T<sub>x</sub>@chitosan films with a 3D ordered porous structure, delivering a capacitance of 245.2 F g<sup>-1</sup> at 2 V s<sup>-1</sup> with a high mass loading of 4 mg cm<sup>-2</sup> of chitosan.<sup>217</sup> An environmentally friendly plasticised electrolyte made from chitosan, potato starch, NH<sub>4</sub>SCN, and glycerol showed a specific capacitance of 16.1 F g<sup>-1</sup>.<sup>218</sup> Additionally, a blend of chitosan, methylcellulose, and various concentrations of glycerol was selected as a host for the ammonium thiocyanate (NH<sub>4</sub>SCN) dopant salt, resulting in a SC with a specific capacitance of 98.08 F g<sup>-1</sup> at 10 mV s<sup>-1</sup>.<sup>219</sup> Chitosan was also used as an aqueous medium for leaching and sorption experiments on E-waste PCB flakes, resulting in the formation of self-N-doped porous carbon with copper oxide nanoparticles. The resultant material, consisting of copper and copper oxide nanoparticles supported by carbon, was mixed with carbon black and PVDF to create an electrode material. The fabricated Li-ion batteries demonstrated a specific capacity of 988 mA h g<sup>-1</sup> during the initial cycle and a 265 mA h g<sup>-1</sup> even after 130 cycles at 1C as seen in Fig. 7(d).<sup>211</sup>

## 4. Challenges and outlook

To better illustrate the performance, the electrochemical mechanisms of the biodegradable biopolymers have been summarized in Table 7 with key highlights of their performance in various studies. Biodegradable biopolymers such as cellulose, shellac, PLA, chitin, and chitosan are a rapidly evolving research field with great potential, but they also present notable challenges and it include.

(a) Cellulose separation and purification of individual biopolymer components often prove difficult and can incur substantial costs, employ hazardous chemicals (alkaline, and bisulphite), or high-energy mechanical means (1000 kW per ton of pulp). Also, CNF derived from cellulose use toxic chemicals such as oxalic acid, acetic acid, or sulfuric, nitric, and hydrochloric acids.



Table 7 Electrochemical performances of biodegradable polymer based devices

Device & component	Materials	Methods	Electrochemical performance	Ref.
<b>Cellulose</b>				
Paper SC & bilayer separator	Water hyacinth CNF/PEG/PVA	Freeze-thawing/NIPS	Ionic conductivity ~ 0.52 mS cm <sup>-1</sup>	149
Aqueous zinc-ion batteries & sulfonated cellulose separator	Cotton cellulose fibre/sulphur trioxide pyridine complex	Freeze dried/pressing	Life cycle- 2500 and 1200 hours at 1 and 4 mA h cm <sup>-2</sup>	128
Li-S battery & Woven separator	PAN/cellulose fibre	Electrospinning	Specific capacity of 4.0 mA h cm <sup>-2</sup> after 200 cycles	150
Symmetrical SC & separator	Rice straw-derived cellulose nanofibril/PDMAC	TEMPO-oxidised/sonication	CNF membrane resulted in a 1.2–1.4 times increase in energy and power densities	129
Sodium metal battery & separator	Cellulose/polyprrole	Ultrasonicate/polymerisation	Sodium ion transfer (0.62), conductance (2.77 mS cm <sup>-1</sup> )	130
<b>Shellac</b>				
Zinc-air battery & binder	Shellac binder	Planetary mixer	Power density of 150 $\mu$ W cm <sup>-2</sup> at a current of 0.5 mA	156
SC & electrode material	Shellac as graphene source grown on the substrates	Dip coated/heating	Capacitance of 1.7 F cm <sup>-2</sup>	157
SC & electrode material	Shellac as rGO source on paper substrate for SC	Laser irradiations	rGO/Shellac/FR/paper exhibited capacitance 31.25 mF cm <sup>-2</sup>	158
Paper battery & binder	Shellac binder	Mixing/brushing	Power density 359.75 $\mu$ W cm <sup>-2</sup> and 3.35 V maximum output	163
Paper SC & current collector ink	Graphite flakes and carbon-black in shellac	Direct-ink-writing 3D printed	Capacitance of 25.6 F g <sup>-1</sup>	164
<b>PLA</b>				
Micro SC & electrode material	PLA/halloysite nano-clay	Stirring/sonication	197.7 mF g <sup>-1</sup> specific capacitance at 0.45 mA g <sup>-1</sup>	175
Quasi-solid-state SC & gel polymer electrolyte	PLA/PVDF-HEP	Doctor blade	Retaining 83% capacitance at 8 mA cm <sup>-2</sup> and 70% after 10 000 cycles under deformation	176
SC & electrode material	PLA-graphene-cellulose/polyaniline	Electrospinning	Capacitance of 16.54 F g <sup>-1</sup> at 0.05 A g <sup>-1</sup>	171
Micro SC & electrode material	PLA/poly(4-styrene sulfonate)	Casting	Areal capacitance of 490.3 mF cm <sup>-2</sup> at a 0.3 mA cm <sup>-2</sup>	172
Flexible solid-state SC & electrode material	PLA/graphite/poly(ethylene glycol) monomethyl ether	Film casting	Areal capacitance of 10 mF cm <sup>-2</sup> at 0.15 mA cm <sup>-2</sup>	173
<b>Chitosan</b>				
SC & nanohybrid membrane	Nano chitosan/nickel oxide nanoparticles	Nano chitosan-freeze-dried/NiO-thermal decomposition	—	204
Lithium–sulfur battery & cathode material	Chitosan powder derived N-doped biochars	Low-temperature pyrolysis	Discharge capacity of 874 mA h g <sup>-1</sup> , dropping to 828 mA h g <sup>-1</sup> in the 2nd cycle	209
EDLC SC & polymer electrolyte	Chitosan/lithium acetate/Glycerol	Magnetic stirrer	Specific capacitance of 132.8 F g <sup>-1</sup> and power density (2591 W kg <sup>-1</sup> )	216
Electrochemical capacitor & nanocomposite film	Chitosan/MnO <sub>2</sub> nanoparticles	One-step electrodeposition	Specific capacitance of 424 F g <sup>-1</sup> at 1 mA cm <sup>-2</sup>	210
Symmetrical SC & 3-D film	Chitosan/2D MXene nanosheet (Ti <sub>3</sub> C <sub>2</sub> T <sub>x</sub> ) film	Freeze-dried	Power density of 143.2 $\mu$ W h cm <sup>-2</sup>	217

(b) Shellac, used as a binder for electrode materials in the fabrication of batteries designed as single-use EESDs, may lack the durability or recharging capability needed for multiple cycling.

(c) Although PLA's production reflects its growing importance and adoption in various industries due to its biodegradability and sustainable production process, its slow degradation

results in long lifetimes but creates problems when it's time to dispose.

(d) Like cellulose, chitin, and chitosan chemical methods of separation have drawbacks, including the use of toxic or corrosive chemicals like HCl and NaOH, which can generate significant environmental pollution.



(e) Synthesis of carbon-based electrode materials from chitin and chitosan have shown excellent performance within the literature; however, this work is mostly experimental, and more work is required for it to be applicable for commercial purposes.

(f) Future trends which are relevant include flexible, wearable, stretchable, and transparent EESDs where biodegradable biopolymers can be incorporated to achieve a closed-loop economy for EESDs. However, a critical issue is the challenge of achieving performances comparable to those of traditional EESDs.

(g) Future development of cellulose, shellac, PLA, chitin, and chitosan binders should consider the ease of disassembly of EESD components through thermal or green solvents for sustainability. These binders support a circular manufacturing approach and enhance the environmental responsibility of the supply chain.

Fig. 8 provides an overview of the outlook for biodegradable biopolymers. The extraction process focuses on achieving efficiency in extraction, encompassing purification, separation, yield, scalability, optimisation, and quality control. These factors are vital to ensuring consistent biopolymer performance in energy storage applications, where high purity and stability are essential for device reliability. Additionally, the sustainability aspects of the extraction process impact environmental considerations, such as waste disposal, toxin management, energy demands, and material degradation. Since biodegradable biopolymers are valued for their eco-friendly properties, minimising environmental costs, reducing toxins, and managing waste are essential for making this technology viable

and aligned with green chemistry principles. Balancing efficiency with sustainability is crucial to optimising biopolymer extraction, making them a responsible and suitable choice for renewable EESD solutions.

Enhancing the structure of biodegradable biopolymers for EESDs emphasises the importance of reinforcing these materials with additional biodegradable components to improve their mechanical and electrochemical properties. Advanced functionalisation techniques, such as crosslinking and refined mixing methods, are crucial for developing a more robust matrix within these materials, resulting in improved stability and performance for energy storage. A major focus is the development of smart biodegradable biopolymer composites, designed to incorporate responsive behaviours or enhanced conductivity. These structural modifications will enhance mechanical strength, biodegradability, and electrochemical efficiency, making biopolymers more suitable for sustainable EESD applications. The design framework emphasises cost-effectiveness as a key factor in selecting biodegradable biopolymers, with targeted modifications to enhance performance and reliability in EESDs. Additionally, integrating machine learning techniques, such as convolutional neural networks (CNN) and long short-term memory (LSTM) models, aids in optimising polymer design. By generating and analysing datasets through these methods, researchers and industries can accelerate the discovery and fine-tuning of material properties, making the design process both more efficient and predictive.

Conventional characterisation techniques, including X-ray diffraction (XRD), scanning electron microscopy (SEM), and X-

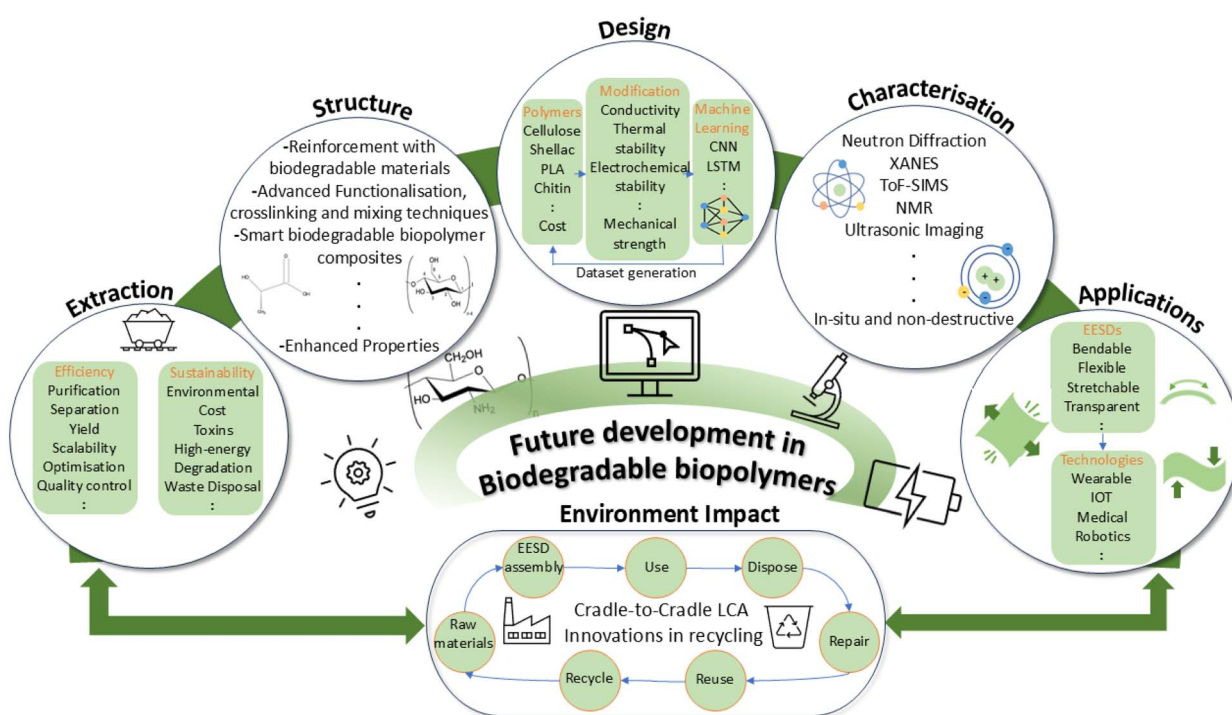


Fig. 8 Research opportunities for biodegradable biopolymers include advancements in extraction processes, structural modifications, AI-driven design, advanced characterisation techniques, and application development. These opportunities aim to enhance environmental sustainability while optimising performance.



ray photoelectron spectroscopy (XPS), are typically conducted *ex situ* and require disassembly of EESDs, which complicates the mechanistic study and ongoing research of biodegradable biopolymer based rechargeable EESDs, often obscuring critical design principles. Recent focus has shifted toward *in situ* and *operando* techniques to help avoid negative effects and uncertainties from sample post-treatment, providing more accurate information about electrochemical processes. Advanced techniques, such as time-of-flight secondary ion mass spectroscopy (TOF-SIMS), are particularly effective for characterising interfacial composition due to their high mass sensitivity and ultrahigh spatial resolution. Deeper insights into atomic and ionic structures can be achieved with aberration-corrected high-angle annular dark-field scanning TEM (HAADF-STEM), neutron diffraction, and X-ray absorption near edge structure (XANES) analysis.

Future applications of EESDs, including bendable, flexible, and stretchable devices like wearables, IoT devices, and medical technologies, will benefit greatly from a balance between environmental sustainability and high EESD performance. A Cradle-to-Cradle life cycle assessment (LCA) for EEDs is an approach focused on designing products with sustainability, reuse, and circularity in mind. Unlike traditional linear LCA models, which often end with disposal, Cradle-to-Cradle LCA promotes a regenerative life cycle where materials are either fully biodegradable or indefinitely recyclable, minimising waste and environmental impact. Cradle-to-Cradle LCA evaluates the sourcing of raw materials, such as biodegradable biopolymers, the energy efficiency of the manufacturing processes, and the longevity and durability of the devices. It further assesses the potential for the device's components to be disassembled, recovered, or repurposed at the end of life, effectively closing the loop. Furthermore, innovating recycling strategies that align with green chemistry principles is essential for the future development of EESDs. Efficient and sustainable recycling practices can significantly reduce waste and environmental pollution associated with EESD disposal. Current EESD recycling approaches as mentioned previously, such as pyrometallurgy, hydrometallurgy, and direct regeneration techniques, primarily target the recovery of valuable elements or materials from the cathode. Moving forward, researchers should prioritise environmentally friendly recycling processes that facilitate the recovery and reuse of all EESD components. These combined efforts will contribute to a more sustainable future for EESDs.

## 5. Conclusions

In the context of batteries and SC, biodegradable biopolymers are vital for the circular economy of EESDs. These materials function as binders, electrode materials, electrolyte materials, polymer solid electrolytes, hydrogels, and separators, amongst others. These eco-friendly materials have low resource consumption in device production and disposal but also possess all the required properties for energy storage. To increase the sustainability and recyclability of batteries and SC, biodegradable biopolymers can be incorporated into the

conception and fabrication of these devices. It also encourages the production of less environmentally hazardous technologies and lowers the CF of the energy storage sector. This paper focuses on cellulose, shellac, PLA, chitin, and chitosan due to their exceptional sustainability, biodegradability, and functional properties with emphasis on their background, processing/preparation techniques, properties, chemical characteristics, usage, and some of the latest research undertaken.

With only 17.4% of E-waste collected and recycled, while the rest deposited as incineration and landfill.<sup>107</sup> This underlines the urgent need to prioritise the use of environmentally friendly and biodegradable biopolymers to achieve a circular economy. Moreover, cellulose and chitosan are the most used biodegradable biopolymers in both battery and SC as shown by the results in Fig. 2. In contrast, shellac is significantly underused, despite its potential as a biodegradable material. This suggests an opportunity for further exploration and development of shellac in energy storage devices, where its unique properties could be used to enhance the sustainability and performance of EESDs. Critical aspects such as efficient extraction, purification, and sustainable recycling methods, aligned with green chemistry principles, are emphasised to ensure environmental responsibility. Key challenges include the high costs and hazardous chemicals involved in purification, durability issues, and limited commercial application. To enhance biodegradable biopolymer performance in EESDs, advanced structural modifications, including reinforcement, crosslinking, and smart biopolymer composites, improve mechanical strength, biodegradability, and electrochemical stability. Machine learning tools, like CNN and LSTM, accelerate design optimisation by generating datasets to refine material properties. *In situ/operando* characterisation techniques, such as TOF-SIM, offer precise insights into electrochemical processes, overcoming the limitations of *ex situ* methods. Future applications, like wearable and flexible devices, will benefit from a Cradle-to-Cradle LCA framework for closed-loop sustainability, supported by evolving recycling methods to recover and reuse all EESD components, fostering a circular economy for sustainable energy storage solutions.

## Data availability

No primary research results, software or code have been included and no new data were generated or analysed as part of this review.

## Author contributions

Libu Manjakkal and Mustehsan Beg: conceptualization, Mustehsan Beg, Jeeva Saju, Keith M. Alcock, Achu Titus Mavelil, Prasutha Rani Markapudi, Hongnian Yu, Libu Manjakkal: methodology, writing – original draft preparation, visualization. Mustehsan Beg and Libu: sorting tables and figures. Hongnian Yu and Libu Manjakkal: reviewing, supervision, reviewing and editing.



## Conflicts of interest

There are no conflicts to declare.

## Acknowledgements

This work was supported by the Edinburgh Napier University SCEBE Starter Grant (N480-000) and The Carnegie Trust for the Universities of Scotland Grant (R2552-00).

## References

- 1 R. Agrawal, S. Agrawal, A. Samadhiya, A. Kumar, S. Luthra and V. Jain, *Geosci. Front.*, 2024, **15**, 101669.
- 2 R. Kumar, D. Lee, Ü. Ağbulut, S. Kumar, S. Thapa, A. Thakur, R. Jilte, C. A. Saleel and S. Shaik, *J. Therm. Anal. Calorim.*, 2024, **149**, 1895–1933.
- 3 N. Saqib, M. Usman, I. Ozturk and A. Sharif, *Energy Policy*, 2024, **184**, 113863.
- 4 O. N. Mishra and B. Prajapati, *IRJAEM*, 2024, **2**, 785–791.
- 5 B. Niu, S. E, Q. Song, Z. Xu, B. Han and Y. Qin, *Nat. Rev. Chem.*, 2024, 1–18.
- 6 J. Köpman and J. Majava, *Resour. Conserv. Recycl. Advances*, 2024, 200207.
- 7 S. Nandy, E. Fortunato and R. Martins, *Prog. Nat. Sci.: Mater. Int.*, 2022, **32**, 1–9.
- 8 L. Manjakkal, A. Pullanchiyodan, N. Yogeswaran, E. S. Hosseini and R. Dahiya, *Adv. Mater.*, 2020, **32**, 1907254.
- 9 A. T. Mavelil, V. Sam, P. R. Markapudi, F. Paul, M. Beg and L. Manjakkal, *IEEE Sens. Lett.*, 2024, **8**, 1–4.
- 10 F. F. Franco, R. A. Hogg and L. Manjakkal, *Biosensors*, 2022, **12**, 174.
- 11 L. Manjakkal, F. F. Franco, A. Pullanchiyodan, M. González-Jiménez and R. Dahiya, *Adv. Sustainable Syst.*, 2021, **5**, 2000286.
- 12 L. Manjakkal, M. Soni, N. Yogeswaran and R. Dahiya, *IEEE FLEPS*, 2019, 1–3.
- 13 Q. Huang, D. Wang and Z. Zheng, *Adv. Energy Mater.*, 2016, **6**, 1600783.
- 14 I. Ali, N. Karim and S. Afroz, *EcoMat*, 2024, e12471.
- 15 M. Azeem, M. Shahid, I. Masin and M. Petru, *J. Text. Inst.*, 2024, 1–16.
- 16 A. M. Soomro, B. Jawed, A. Qayoom, H. Hyder, K. Hussain, L. Iram, M. Waqas, F. Ahmed, A. Sattar and S. Almani, *Phys. Status Solidi A*, 2024, **221**, 2300523.
- 17 C. Hu, F. Wang, X. Cui and Y. Zhu, *Adv. Compos. Hybrid Mater.*, 2023, **6**, 70.
- 18 A. R. Peringath, M. A. H. Bayan, M. Beg, A. Jain, F. Pierini, N. Gadegaard, R. Hogg and L. Manjakkal, *J. Energy Storage*, 2023, **73**, 108811.
- 19 G. Gopinath, S. Ayyasamy, P. Shanmugaraj, R. Swaminathan, K. Subbiah and S. Kandasamy, *J. Energy Storage*, 2023, **70**, 108065.
- 20 W. M. T. Ramya, V. Siva, A. Murugan, A. Shameem, S. Kannan and K. Venkatachalam, *J. Polym. Environ.*, 2023, **31**, 1610–1627.
- 21 J. Gamboa, S. Paulo-Mirasol, F. Estrany and J. Torras, *ACS Appl. Bio Mater.*, 2023, **6**, 1720–1741.
- 22 A. Khezerlou, M. Tavassoli, M. Alizadeh Sani, K. Mohammadi, A. Ehsani and D. J. McClements, *Polymers*, 2021, **13**, 4399.
- 23 N. B. Rathod, S. P. Bangar, V. Šimat and F. Ozogul, *Int. J. Food Sci. Technol.*, 2023, **58**, 854–861.
- 24 A. Thulasisingh, K. Kumar, B. Yamunadevi, N. Poojitha, S. SuhailMadharHanif and S. Kannaiyan, *Polym. Bull.*, 2021, 1–30.
- 25 V. Hernández, D. Ibarra, J. F. Triana, B. Martínez-Soto, M. Faúndez, D. A. Vasco, L. Gordillo, F. Herrera, C. García-Herrera and A. Garmulewicz, *Materials*, 2022, **15**, 3954.
- 26 M. Y. Khalid and Z. U. Arif, *Food Packag. Shelf Life*, 2022, **33**, 100892.
- 27 K. Y. Perera, A. K. Jaiswal and S. Jaiswal, *Foods*, 2023, **12**, 2422.
- 28 J. R. Westlake, M. W. Tran, Y. Jiang, X. Zhang, A. D. Burrows and M. Xie, *Sustainable Food Technol.*, 2023, **1**, 50–72.
- 29 Y. Liu, S. Ahmed, D. E. Sameen, Y. Wang, R. Lu, J. Dai, S. Li and W. Qin, *Trends Food Sci. Technol.*, 2021, **112**, 532–546.
- 30 W. Xue, J. Zhu, P. Sun, F. Yang, H. Wu and W. Li, *Trends Food Sci. Technol.*, 2023, **136**, 295–307.
- 31 L. Pinto, M. A. Bonifacio, E. De Giglio, E. Santovito, S. Cometa, A. Bevilacqua and F. Baruzzi, *Food Packag. Shelf Life*, 2021, **28**, 100676.
- 32 J. C. Abdullah, M. A. Hafeez, Q. Wang, S. Farooq, Q. Huang, W. Tian and J. Xiao, *Front. Nutr.*, 2022, **9**, 1000116.
- 33 P. Ezati, A. Khan, R. Priyadarshi, T. Bhattacharya, S. K. Tammina and J.-W. Rhim, *Food Hydrocolloids*, 2023, **142**, 108771.
- 34 R. Priyadarshi, S. Roy, T. Ghosh, D. Biswas and J.-W. Rhim, *Sustainable Mater. Technol.*, 2022, **32**, e00353.
- 35 Z. Tariq, D. N. Iqbal, M. Rizwan, M. Ahmad, M. Faheem and M. Ahmed, *RSC Adv.*, 2023, **13**, 24731–24754.
- 36 R. Phiri, S. M. Rangappa, S. Siengchin, O. P. Oladijo and H. N. Dhakal, *Adv. Ind. Eng. Polym. Res.*, 2023, **6**(4), 436–450.
- 37 S. Birania, S. Kumar, N. Kumar, A. K. Attkan, A. Panghal, P. Rohilla and R. Kumar, *J. Food Process Eng.*, 2022, **45**, e13930.
- 38 D. Puglia, D. Pezzolla, G. Gigliotti, L. Torre, M. L. Bartucca and D. Del Buono, *Sustainability*, 2021, **13**, 2710.
- 39 R. Saberi Riseh, M. Gholizadeh Vazvani, M. Hassanisaadi and Y. A. Skorik, *Polymers*, 2023, **15**, 440.
- 40 M. A. M. Akhir and M. Mustapha, *Polym. Rev.*, 2022, **62**, 890–918.
- 41 T. Pirzada, B. V. de Farias, R. Mathew, R. H. Guenther, M. V. Byrd, T. L. Sit, L. Pal, C. H. Opperman and S. A. Khan, *Curr. Opin. Colloid Interface Sci.*, 2020, **48**, 121–136.
- 42 T. O. Machado, J. Grabow, C. Sayer, P. H. de Araújo, M. L. Ehrenhard and F. R. Wurm, *Adv. Colloid Interface Sci.*, 2022, **303**, 102645.
- 43 J. Baranwal, B. Barse, A. Fais, G. L. Delogu and A. Kumar, *Polymers*, 2022, **14**, 983.

44 S.-B. Park, M.-H. Sung, H. Uyama and D. K. Han, *Prog. Polym. Sci.*, 2021, **113**, 101341.

45 G. P. Udayakumar, S. Muthusamy, B. Selvaganesh, N. Sivarajasekar, K. Rambabu, F. Banat, S. Sivamani, N. Sivakumar, A. Hosseini-Bandegharaei and P. L. Show, *J. Environ. Chem. Eng.*, 2021, **9**, 105322.

46 R. Velu, D. K. Jayashankar and K. Subburaj, in *Additive Manufacturing*, Elsevier, 2021, pp. 635–659.

47 N. Kučuk, M. Primožič, Ž. Knez and M. Leitgeb, *Int. J. Mol. Sci.*, 2023, **24**, 3188.

48 D. Veeman, M. S. Sai, P. Sureshkumar, T. Jagadeesha, L. Natrayan, M. Ravichandran and W. D. Mammo, *Int. J. Polym. Sci.*, 2021, **2021**, 4907027.

49 K. Varma and S. Gopi, in *Biopolymers and Their Industrial Applications*, Elsevier, 2021, pp. 175–191.

50 T. Monia, *J. Thermoplast. Compos. Mater.*, 2024, **37**, 2505–2524.

51 A. Jahandideh, M. Ashkani and N. Moini, in *Biopolymers and Their Industrial Applications*, Elsevier, 2021, pp. 193–218.

52 M. Daria, L. Krzysztof and M. Jakub, *J. Cleaner Prod.*, 2020, **268**, 122129.

53 F. H. H. Abdellatif and M. M. Abdellatif, in *Green Chemistry for Sustainable Textiles*, Elsevier, 2021, pp. 453–469.

54 A. Patti and D. Acierno, *Polymers*, 2022, **14**, 692.

55 A. Elamri, K. Zdiri, M. Hamdaoui and O. Harzallah, *Text. Res. J.*, 2023, **93**, 1456–1484.

56 X. Peng, M. Umer, M. N. Pervez, K. F. Hasan, M. A. Habib, M. S. Islam, L. Lin, X. Xiong, V. Naddeo and Y. Cai, *Case Stud. Chem. Environ. Eng.*, 2023, **7**, 100349.

57 S. Kopf, D. Åkesson and M. Skrifvars, *Polym. Rev.*, 2023, **63**, 200–245.

58 N. Vrinceanu, S. Bucur, C. M. Rimbu, S. Neculai-Valeanu, S. Ferrandiz Bou and M. P. Sucheia, *Text. Res. J.*, 2022, **92**, 3889–3902.

59 S. K. Awasthi, M. Kumar, V. Kumar, S. Sarsaiya, P. Anerao, P. Ghosh, L. Singh, H. Liu, Z. Zhang and M. K. Awasthi, *Environ. Pollut.*, 2022, **307**, 119600.

60 E. M. Polman, G.-J. M. Gruter, J. R. Parsons and A. Tietema, *Sci. Total Environ.*, 2021, **753**, 141953.

61 I. Surya, E. Chong, H. A. Khalil, O. G. Funmilayo, C. Abdullah, N. S. Aprilia, N. Olaiya, T. Lai and A. Oyekanmi, *J. Mater. Res. Technol.*, 2021, **12**, 1673–1688.

62 S. E. Mousavi Kalajahi, A. Alizadeh, H. Hamishehkar, H. Almasi and N. Asefi, *J. Polym. Environ.*, 2022, **30**, 258–269.

63 R. T. Abdulwahid, S. B. Aziz and M. F. Kadir, *Mater. Today Sustain.*, 2023, **23**, 100472.

64 Z. Wang, Z. Ma, J. Sun, Y. Yan, M. Bu, Y. Huo, Y.-F. Li and N. Hu, *Polymers*, 2021, **13**, 813.

65 C. Cui, Q. Fu, L. Meng, S. Hao, R. Dai and J. Yang, *ACS Appl. Bio Mater.*, 2020, **4**, 85–121.

66 S. Jafarzadeh and S. M. Jafari, *Crit. Rev. Food Sci. Nutr.*, 2021, **61**, 2640–2658.

67 C. J. Chirayil, A. M. Joseph, J. Joy, T. Unnikrishnan and S. Thomas, in *Handbook of Natural Polymers*, Elsevier, 2024, vol. 2, pp. 427–451.

68 S. Torgbo and P. Sukyai, *Polym. Degrad. Stab.*, 2020, **179**, 109232.

69 G. Fredi and A. Pegoretti, It Is Supported by the European Commission under the Erasmus+ Programme. However, the European Commission and the Turkish National Agency Cannot Be Held Responsible for the Opinions Contained Herein, 2024, vol. 242.

70 J. Lal, S. K. Singh, P. Biswas, A. Vaishnav, N. K. Yadav and S. Chandravanshi, in *Advanced Strategies for Biodegradation of Plastic Polymers*, Springer, 2024, pp. 283–301.

71 R. Rajesh, *i-Manager's Journal on Material Science*, 2023, **11**, 14–22.

72 C. F. Soon, S. K. Yee, A. N. Nordin, R. A. Rahim, N. L. Ma, I. S. L. A. Hamed, K. S. Tee, N. H. Azmi, N. M. Sunar and C. Heng, *Int. J. Precis. Eng. Manuf.*, 2024, 1–30.

73 A. Géczy, C. Farkas, R. Kovács, D. Froš, P. Veselý and A. Bonyár, *IEEE Open J. Nanotechnol.*, 2022, **3**, 182–190.

74 A. Yedrissov, D. Khrustalev, A. Alekseev, A. Khrustaleva and A. Vetrova, *Mater. Today: Proc.*, 2022, **49**, 2443–2448.

75 B. L. Turner, J. Twiddy, M. D. Wilkins, S. Ramesh, K. M. Kilgour, E. Domingos, O. Nasrallah, S. Menegatti and M. A. Daniele, *npj Flexible Electron.*, 2023, **7**, 25.

76 A. Géczy, A. Csiszár, E. Rozs, I. Hajdu, B. Medgyes, O. Krammer and D. Straubinger, *IEEE Xplore*, 2022, 1–6.

77 H. István, H. Amír, L. P. Tamás and G. Attila, *IEEE Xplore*, 2024, 1–5.

78 K. Nath, S. K. Bhattacharyya and N. C. Das, in *Materials for Potential EMI Shielding Applications*, Elsevier, 2020, pp. 165–178.

79 Z. Zhai, X. Du, Y. Long and H. Zheng, *Front. Electron.*, 2022, **3**, 985681.

80 I. N. Vikhareva, E. A. Buylova, G. U. Yarmuhamedova, G. K. Aminova and A. K. Mazitova, *J. Chem.*, 2021, **2021**, 5099705.

81 E. Lizundia and D. Kundu, *Adv. Funct. Mater.*, 2021, **31**, 2005646.

82 J. Barbosa, A. Reizabal, D. Correia, A. Fidalgo-Marijuan, R. Gonçalves, M. Silva, S. Lanceros-Mendez and C. Costa, *Mater. Today Energy*, 2020, **18**, 100494.

83 G. Palanisamy, S. Thangarasu, R. K. Dharman, C. S. Patil, T. P. P. S. Negi, M. D. Kurkuri, R. K. Pai and T. H. Oh, *J. Energy Chem.*, 2023, **80**, 402–431.

84 N. M. Ghazali and A. S. Samsudin, *Mater. Today: Proc.*, 2022, **49**, 3668–3678.

85 T. Xu, K. Liu, N. Sheng, M. Zhang, W. Liu, H. Liu, L. Dai, X. Zhang, C. Si and H. Du, *Energy Storage Mater.*, 2022, **48**, 244–262.

86 E. S. Appiah, P. Dzikunu, N. Mahadeen, D. N. Ampong, K. Mensah-Darkwa, A. Kumar, R. K. Gupta and M. Adom-Asamoah, *Molecules*, 2022, **27**, 6556.

87 R. Vinodh, Y. Sasikumar, H.-J. Kim, R. Atchudan and M. Yi, *J. Ind. Eng. Chem.*, 2021, **104**, 155–171.

88 T. Zhang, J. Wu, Y. Wang, L. Zhang and F. Ran, *Adv. Energy Mater.*, 2024, **14**, 2303587.

89 S. Ahmed, P. Sharma, S. Bairagi, N. P. Rumjit, S. Garg, A. Ali, C. W. Lai, S. M. Mousavi, S. A. Hashemi and C. M. Hussain, *J. Energy Storage*, 2023, **66**, 107391.

90 L. Manjakkal, A. Jain, S. Nandy, S. Goswami, J. Tiago Carvalho, L. Pereira, C. H. See, S. C. Pillai and R. A. Hogg, *Chem. Eng. J.*, 2023, **465**, 142845.

91 S. Nandy, S. Goswami, A. Marques, D. Gaspar, P. Grey, I. Cunha, D. Nunes, A. Pimentel, R. Igreja, P. Barquinha, L. Pereira, E. Fortunato and R. Martins, *Adv. Mater. Technol.*, 2021, **6**, 2000994.

92 P. C. Ani, P. U. Nzereogu, A. C. Agbogu, F. I. Ezema and A. C. Nwanya, *Appl. Surf. Sci. Adv.*, 2022, **11**, 100298.

93 C. Yan, F. Shan, X. Ying and Z. Li, *Chin. Med. J.*, 2023, **136**, 397–406.

94 UNEP, *E-waste: inventory assessment manual*, 2007.

95 A. L. Srivastav, Markandeya, N. Patel, M. Pandey, A. K. Pandey, A. K. Dubey, A. Kumar, A. K. Bhardwaj and V. K. Chaudhary, *Environ. Sci. Pollut. Res.*, 2023, **30**, 48654–48675.

96 S. T. Ghulam and H. Abushammala, *Sustainability*, 2023, **15**, 1837.

97 J. Wu, M. Zheng, T. Liu, Y. Wang, Y. Liu, J. Nai, L. Zhang, S. Zhang and X. Tao, *Energy Storage Mater.*, 2023, **54**, 120–134.

98 S. Mir and N. Dhawan, *Miner. Process. Extr. Metall.*, 2022, **132**, 87–98.

99 M. Agrawal, R. Singh, M. Ranitović, Z. Kamberovic, C. Ekberg and K. K. Singh, Global market trends of tantalum and recycling methods from Waste Tantalum Capacitors: A review, *Sustainable Mater. Technol.*, 2021, **29**, e00323.

100 Y. Zhao, Y. Kang, J. L. John Wozny, H. Du, C. Li, T. Li, F. Kang, N. Tavajohi and B. Li, *Nat. Rev. Mater.*, 2023, **8**, 623–634.

101 G. Yuan, X. Liu, C. Zhang, D. T. Pham and Z. Li, *Eng. Appl. Artif. Intell.*, 2023, **126**(106878).

102 Y. Lin, Z. Yu, Y. Wang and M. Goh, *J. Environ. Manage.*, 2023, **332**(117354).

103 H. Trivedi, K. D. Verma and K. K. Kar, *Recycling of Supercapacitor Materials*, Springer International Publishing, 2023, pp. 393–411, DOI: [10.1007/978-3-031-23701-0\\_16](https://doi.org/10.1007/978-3-031-23701-0_16).

104 G. Jiang and S. J. Pickering, *Waste Biomass Valorization*, 2019, **10**, 215–221.

105 F. Mashkoor, R. Mashkoor, M. Shoeb, A. H. Anwer, M. Z. Ansari and C. Jeong, *Appl. Clay Sci.*, 2023, **245**, 107149.

106 E. Fan, L. Li, Z. Wang, J. Lin, Y. Huang, Y. Yao, R. Chen and F. Wu, *Chem. Rev.*, 2020, **120**, 7020–7063.

107 H.-X. Kuang, M.-Y. Li, L.-Z. Li, Z.-C. Li, C.-H. Wang, M.-D. Xiang and Y.-J. Yu, *Sci. Total Environ.*, 2023, **863**, 160911.

108 C. M. Costa, J. C. Barbosa, R. Gonçalves, H. Castro, F. Del Campo and S. Lanceros-Méndez, *Energy Storage Mater.*, 2021, **37**, 433–465.

109 H. Yu, H. Dai, G. Tian, B. Wu, Y. Xie, Y. Zhu, T. Zhang, A. M. Fathollahi-Fard, Q. He and H. Tang, *Renewable Sustainable Energy Rev.*, 2021, **135**, 110129.

110 J. Zheng and S. Suh, *Nat. Clim. Change*, 2019, **9**, 374–378.

111 X. Sun, X. Pei, Y. Yang, Y. Bai and R. Li, *Ind. Crops Prod.*, 2024, **214**, 118596.

112 P. G. Ponnusamy and S. Mani, *Int. J. Life Cycle Assess.*, 2022, **27**, 380–394.

113 F. A. Vicente, R. Hren, U. Novak, L. Čuček, B. Likozar and A. Vujanović, *Renewable Sustainable Energy Rev.*, 2024, **192**, 114204.

114 M. Berroci, C. Vallejo and E. Lizundia, *ACS Sustain. Chem. Eng.*, 2022, **10**, 14280–14293.

115 C. Ingrao, C. Tricase, A. Cholewa-Wójcik, A. Kawecka, R. Rana and V. Siracusa, *Sci. Total Environ.*, 2015, **537**, 385–398.

116 J. L. Wang, J. K. Xu, C. Hopkins, D. H. K. Chow and L. Qin, *Adv. Sci.*, 2020, **7**, 1902443.

117 D. Klemm, B. Heublein, H.-P. F. habil and A. Bohn, *Angew. Chem., Int. Ed.*, 2005, **44**, 3358–3393.

118 T. Heinze, *Cellulose Chemistry and Properties: Fibers, Nanocelluloses and Advanced Materials*, Springer, Switzerland, 2016.

119 T. Heinze and T. Liebert, *Celluloses and polyoses/hemicelluloses*, 2012, pp. 83–152.

120 R. A. Young, *Cellulose*, 1994, **1**, 107–130.

121 B. Wang, M. Sain and K. Oksman, *Appl. Compos. Mater.*, 2007, **14**, 89–103.

122 J. P. S. Morais, M. de Freitas Rosa, L. D. Nascimento, D. M. Do Nascimento and A. R. Cassales, *Carbohydr. Polym.*, 2013, **91**, 229–235.

123 E. de Moraes Teixeira, A. C. Corrêa, A. Manzoli, F. de Lima Leite, C. R. de Oliveira and L. H. C. Mattoso, *Cellulose*, 2010, **17**, 595–606.

124 E. Abraham, B. Deepa, L. A. Pothan, M. Jacob, S. Thomas, U. Cvelbar and R. Anandjiwala, *Carbohydr. Polym.*, 2011, **86**, 1468–1475.

125 A. Alemdar and M. Sain, *Bioresour. Technol.*, 2008, **99**, 1664–1671.

126 A. Thygesen, J. Oddershede, H. Lilholt, A. B. Thomsen and K. Ståhl, *Cellulose*, 2005, **12**, 563–576.

127 S. Eyley and W. Thielemans, *Nanoscale*, 2014, **6**, 7764–7779.

128 W. Zhou, M. Yang, M. Chen, G. Zhang, X. Han, J. Chen, D. Ma and P. Zhang, *Adv. Funct. Mater.*, 2024, **34**, 2315444.

129 M. A. Islam, H. L. Ong, N. A. A. Sezali, C.-K. Tsai and R.-A. Doong, *J. Power Sources*, 2024, **614**, 234965.

130 S. Deng, W. Meng, C. Fan, D. Zuo, J. Han, T. Li, D. Li and L. Jiang, *ACS Appl. Mater. Interfaces*, 2024, **16**, 4708–4718.

131 A. C. O'sullivan, *Cellulose*, 1997, **4**, 173–207.

132 B. Lindman, G. Karlström and L. Stigsson, *J. Mol. Liq.*, 2010, **156**, 76–81.

133 C. J. Biermann, *Handbook of Pulping and Papermaking*, 1996, vol. 2, pp. 13–50.

134 R. Li, Y. Zheng, X. Zhao, Q. Yong, X. Meng, A. J. Ragauskas and C. Huang, *Green Chem.*, 2023, 2505–2523.

135 P. Bajpai, *Biotechnology for Pulp and Paper Processing*, Springer, 2012.

136 S. S. Department, Production of pulp for paper worldwide in 2021, by type (in 1,000 metric tons), Statista, 2021.

137 N. P. Cheremisinoff and P. E. Rosenfeld, *Handbook of Pollution Prevention and Cleaner Production Vol. 2: Best Practices in the Wood and Paper Industries*, William Andrew, 2009.

138 S. Peter, N. Lyczko, D. Gopakumar, H. J. Maria, A. Nzihou and S. Thomas, *J. Mater. Sci.*, 2022, **57**, 6835–6880.

139 X. Fu, T. Sotani and H. Matsuyama, *Desalination*, 2008, **233**, 10–18.

140 T. Omura, T. Suzuki and H. Minami, *Langmuir*, 2020, **36**, 14076–14082.

141 T. G. Van De Ven and A. Sheikhi, *Nanoscale*, 2016, **8**, 15101–15114.

142 W.-C. Li, C.-H. Lin, C.-C. Ho, T.-T. Cheng, P.-H. Wang and T.-C. Wen, *J. Taiwan Inst. Chem. Eng.*, 2022, **133**, 104263.

143 A. Rajeh, M. Morsi and I. Elashmawi, *Vacuum*, 2019, **159**, 430–440.

144 E. Karaca, K. Pekmez and N. Ö. Pekmez, *Electrochim. Acta*, 2018, **273**, 379–391.

145 S. Yang, Y. Huang, S. Su, G. Han and J. Liu, *Powder Technol.*, 2019, **351**, 203–211.

146 C.-U. Jeong, N. Umirov, D.-H. Jung, D.-H. Seo, B.-M. Lee, B.-S. Choi, S.-S. Kim and J.-H. Choi, *J. Power Sources*, 2021, **506**, 230050.

147 Z. Karkar, D. Guyomard, L. Roué and B. Lestriez, *Electrochim. Acta*, 2017, **258**, 453–466.

148 M. Beg, D. Sun, C. M. Popescu, K. M. Alcock, A. J. Onyianta, D. O'Rourke, K. Goh and H. Yu, 2021 *26th International Conference on Automation and Computing: System Intelligence through Automation and Computing*, ICAC, 2021, DOI: [10.23919/ICAC50006.2021.9594191](https://doi.org/10.23919/ICAC50006.2021.9594191).

149 M. Beg, K. M. Alcock, A. Titus Mavelil, D. O'Rourke, D. Sun, K. Goh, L. Manjakkal and H. Yu, *ACS Appl. Mater. Interfaces*, 2023, **15**, 51100–51109.

150 H. Mao, X. Da, H. Shen, W. Zhao, X. Li, Y. Su, S. Ding and W. Yu, *Electrochim. Acta*, 2024, **492**, 144363.

151 J. Selinger, M. T. Islam, Q. Abbas, J. B. Schaubeder, J. Zoder, A. Bakhshi, W. Bauer, M. Hummel and S. Spirk, *Carbohydr. Polym.*, 2024, 122354.

152 Y. Fang, Z. Zhang, S. Liu, Y. Pei and X. Luo, *Electrochim. Acta*, 2024, **475**, 143661.

153 N. Thombare, S. Kumar, U. Kumari, P. Sakare, R. K. Yogi, N. Prasad and K. K. Sharma, *Int. J. Biol. Macromol.*, 2022, **215**, 203–223.

154 Y. Yuan, N. He, Q. Xue, Q. Guo, L. Dong, M. H. Haruna, X. Zhang, B. Li and L. Li, *Trends Food Sci. Technol.*, 2021, **109**, 139–153.

155 K. Rashid Sulthan, S. Hema, G. U. Chandran, M. Sajith, V. Ananthika and S. Sambhudevan, in *Handbook of Biomass*, Springer, 2023, pp. 1–26.

156 A. Poulin, X. Aeby and G. Nyström, *Sci. Rep.*, 2022, **12**, 11919.

157 R. S. Singh, M. Jansen, D. Ganguly, G. U. Kulkarni, S. Ramaprabhu, S. K. Choudhary and C. Pramanik, *Renewable Energy*, 2022, **181**, 1008–1022.

158 P. S. Kumar, S. Vanmathi, H. Awasthi, I. Khan, R. K. Singh, V. K. Sharma, C. Pramanik and S. Goel, *Mater. Adv.*, 2024, **5**, 5932–5944.

159 S. Kumar, A. Sharma, L. Cherwoo, N. Thombare and A. P. Bhondekar, *Kuwait J. Sci.*, 2024, **51**, 100138.

160 K. Sharma, A. R. Chowdhury and S. Srivastava, *Natural Materials and Products from Insects: Chemistry and Applications*, 2020, pp. 21–37.

161 P. Mandal and J. Sarkhel, *Business Spectrum*, 2014, vol. 4, pp. 35–44.

162 J. Derry, *A study on the processing methods of shellac and the analysis of selected physical and chemical characteristics*, University of Oslo Oslo, Norway, 2012.

163 Y. Shi and Y. Wang, Development of a Biodegradable Hybrid Inspired Paper Battery Powered By Carbon-Black with Origami Design Applicable for Biomedical Smart Systems, in *2024 IEEE 3rd International Conference on Computing and Machine Intelligence (ICMI)*, IEEE, 2024, pp. 1–6.

164 X. Aeby, A. Poulin, G. Siqueira, M. K. Hausmann and G. Nyström, *Adv. Mater.*, 2021, **33**, 2101328.

165 K. J. Jem and B. Tan, *Adv. Ind. Eng. Polym. Res.*, 2020, **3**, 60–70.

166 S. Farah, D. G. Anderson and R. Langer, *Adv. Drug Delivery Rev.*, 2016, **107**, 367–392.

167 E. R. Rezvani Ghomi, F. Khosravi, A. S. Saedi Ardahaei, Y. Dai, R. E. Neisiany, F. Foroughi, M. Wu, O. Das and S. Ramakrishna, *Polymers*, 2021, **13**, 1854.

168 F. Carrasco, P. Pagès, J. Gámez-Pérez, O. Santana and M. L. Maspoch, *Polym. Degrad. Stab.*, 2010, **95**, 116–125.

169 L.-T. Lim, R. Auras and M. Rubino, *Prog. Polym. Sci.*, 2008, **33**, 820–852.

170 R. Auras, B. Harte and S. Selke, *Macromol. Biosci.*, 2004, **4**, 835–864.

171 H. Zhu and Y. Xie, *Mater. Today Chem.*, 2023, **30**, 101535.

172 B. S. Chikkatti, A. M. Sajjan, P. B. Kalahal, N. R. Banapurmath and N. H. Ayachit, *J. Energy Storage*, 2023, **72**, 108513.

173 C. Jellett, K. Ghosh, M. P. Browne, V. Urbanova and M. Pumera, *ACS Appl. Energy Mater.*, 2021, **4**, 6975–6981.

174 N.-A. A. B. Taib, M. R. Rahman, D. Huda, K. K. Kuok, S. Hamdan, M. K. B. Bakri, M. R. M. B. Julaihi and A. Khan, *Polym. Bull.*, 2023, **80**, 1179–1213.

175 B. S. Chikkatti, A. M. Sajjan, N. R. Banapurmath, J. K. Bhutto, R. Verma and T. M. Yunus Khan, *Polymers*, 2023, **15**, 4587.

176 C. Yang, Y. Bai, H. Xu, M. Li, Z. Cong, H. Li, W. Chen, B. Zhao and X. Han, *Polymers*, 2022, **14**, 1881.

177 H. Liang, T. Lin and J. Li, *Preparation and Electrochemical Stabilities Study of Graphene/Polyaniline Composites with Polylactic Acid as Biodegradable Adhesive*, 2024.

178 S. Molla, F. Khatun and P. Thakur, *J. Mater. Sci.: Mater. Electron.*, 2022, **33**, 1864–1870.

179 P. Wuamprakhon, R. D. Crapnell, E. Sigley, N. J. Hurst, R. J. Williams, M. Sawangphruk, E. M. Keefe and C. E. Banks, *Adv. Sustainable Syst.*, 2023, **7**, 2200407.

180 C. Reyes, R. Somogyi, S. Niu, M. A. Cruz, F. Yang, M. J. Catenacci, C. P. Rhodes and B. J. Wiley, *ACS Appl. Energy Mater.*, 2018, **1**, 5268–5279.



181 B. T. Iber, N. A. Kasan, D. Torsabo and J. W. Omuwa, *J. Renewable Mater.*, 2022, **10**, 1097.

182 L. Bai, L. Liu, M. Esquivel, B. L. Tardy, S. Huan, X. Niu, S. Liu, G. Yang, Y. Fan and O. J. Rojas, *Chem. Rev.*, 2022, **122**, 11604–11674.

183 D. Kumar and M. Shahid, *Natural Materials and Products from Insects: Chemistry and Applications*, Springer, 2020.

184 S. Peter, N. Lyczko, D. Gopakumar, H. J. Maria, A. Nzihou and S. Thomas, *Waste Biomass Valorization*, 2021, **12**, 4777–4804.

185 A. Anitha, S. Sowmya, P. S. Kumar, S. Deepthi, K. Chennazhi, H. Ehrlich, M. Tsurkan and R. Jayakumar, *Prog. Polym. Sci.*, 2014, **39**, 1644–1667.

186 D. Kasprzak, C. C. Mayorga-Martinez, O. Alduhaish and M. Pumera, *Energy Technol.*, 2023, **11**, 2201103.

187 R. Hao, Y. Yang, H. Wang, B. Jia, G. Ma, D. Yu, L. Guo and S. Yang, *Nano Energy*, 2018, **45**, 220–228.

188 T. Jin, T. Liu, E. Lam and A. Moores, Chitin and chitosan on the nanoscale, *Nanoscale Horiz.*, 2021, **6**, 505–542.

189 P. L. Chee, T. Sathasivam, Y. C. Tan, W. Wu, Y. Leow, Q. R. T. Lim, P. Y. M. Yew, Q. Zhu and D. Kai, *Nanoscale*, 2024, **16**, 3269–3292.

190 Y. Wang, T. Xu, K. Liu, M. Zhang, X. M. Cai and C. Si, *Aggregate*, 2024, **5**, e428.

191 H. Xu and X. Zhao, *ChemSusChem*, 2024, e202400757.

192 T.-W. Zhang, B. Shen, H.-B. Yao, T. Ma, L.-L. Lu, F. Zhou and S.-H. Yu, *Nano Lett.*, 2017, **17**, 4894–4901.

193 T. Zhang, X. Yu, K. Chen, J. Cheng, F. Xiong, X. Zhang, Z. Hou, X. Ma and Z. Zi, *Scr. Mater.*, 2024, **242**, 115951.

194 D. Ruiz, V. F. Michel, M. Niederberger and E. Lizundia, *Small*, 2023, **19**, 2303394.

195 M. Latifi, A. Ahmad, N. H. Hassan and H. Kaddami, *Carbohydr. Polym.*, 2021, **273**, 118542.

196 Y. Wang, R. Liu, Y. Tian, Z. Sun, Z. Huang, X. Wu and B. Li, *Chem. Eng. J.*, 2020, **384**, 123263.

197 M. Luo, Z. Zhu, K. Yang, P. Yang, Y. Miao, M. Chen, W. Chen and X. Zhou, *Sci. Total Environ.*, 2020, **747**, 141923.

198 Z. Shang, X. An, L. Liu, J. Yang, W. Zhang, H. Dai, H. Cao, Q. Xu, H. Liu and Y. Ni, *Carbohydr. Polym.*, 2021, **251**, 117107.

199 C. J. Raj, M. Rajesh, R. Manikandan, K. H. Yu, J. Anusha, J. H. Ahn, D.-W. Kim, S. Y. Park and B. C. Kim, *J. Power Sources*, 2018, **386**, 66–76.

200 B. Duan, X. Gao, X. Yao, Y. Fang, L. Huang, J. Zhou and L. Zhang, *Nano Energy*, 2016, **27**, 482–491.

201 I. Younes and M. Rinaudo, *Mar. Drugs*, 2015, **13**, 1133–1174.

202 T. J. Madera-Santana, C. H. Herrera-Méndez and J. R. Rodríguez-Núñez, *Green Mater.*, 2018, **6**, 131–142.

203 K. Ogawa, T. Yui and K. Okuyama, *Int. J. Biol. Macromol.*, 2004, **34**, 1–8.

204 N. M. El-Shafai, M. Shukry, S. W. Sharshir, M. S. Ramadan, A. Alhadhrami and I. El-Mehasseb, *J. Energy Storage*, 2022, **50**, 104626.

205 S. G. Kou, L. M. Peters and M. R. Mucalo, *Int. J. Biol. Macromol.*, 2021, **169**, 85–94.

206 S. M. Joseph, S. Krishnamoorthy, R. Paranthaman, J. Moses and C. Anandharamakrishnan, *Carbohydr. Polym. Technol. Appl.*, 2021, **2**, 100036.

207 A. Pellis, G. M. Guebitz and G. S. Nyanhongo, *Gels*, 2022, **8**, 393.

208 K. Okuyama, K. Noguchi, M. Kanenari, T. Egawa, K. Osawa and K. Ogawa, *Carbohydr. Polym.*, 2000, **41**, 237–247.

209 R. Nisticò, F. Guerretta, P. Benzi and G. Magnacca, *Int. J. Biol. Macromol.*, 2020, **164**, 1825–1831.

210 S. Hassan, M. Suzuki and A. Abd El-Moneim, *J. Power Sources*, 2014, **246**, 68–73.

211 M. Manickasundaram, K. Lakshmanan, K. Vediappan and S. Kancharla, *Chem. Eng. J.*, 2024, **484**, 149605.

212 H. Ibrahim and E. El-Zairy, *Concepts, Compounds and the Alternatives of Antibacterials*, 2015, vol. 1, pp. 81–101.

213 Y. Ohya, M. Shiratani, H. Kobayashi and T. Ouchi, *J. Macromol. Sci., Part A*, 1994, **31**(5), 629–642.

214 K. Divya and M. Jisha, *Environ. Chem. Lett.*, 2018, 101–112.

215 G. Kravanja, M. Primožič, Ž. Knez and M. Leitgeb, *Molecules*, 2019, **24**, 1960.

216 A. S. Asnawi, S. B. Aziz, M. M. Nofal, M. H. Hamsan, M. A. Brza, Y. M. Yusof, R. T. Abdulwahid, S. K. Muzakir and M. F. Kadir, *Polymers*, 2020, **12**, 1433.

217 Y. Ding, Y. Liu, X. Sun, Y. Yao, B. Yuan, T. Huang and J. Tang, *Chem. Eng. J.*, 2022, **442**, 136255.

218 R. T. Abdulwahid, S. B. Aziz and M. F. Kadir, *J. Energy Storage*, 2023, **67**, 107636.

219 S. B. Aziz, A. S. Asnawi, M. F. Z. Kadir, S. M. Alshehri, T. Ahamad, Y. M. Yusof and J. M. Hadi, *Polymers*, 2021, **13**, 1183.

